TOPICAL REVIEW — Precision measurement and cold matters

High-precision spectroscopy of hydrogen molecular ions*

Zhong Zhen-Xiang(钟振祥)[a], Tong Xin(童 昕)[a], Yan Zong-Chao(严宗朝)[a,b,c]†, and Shi Ting-Yun(史庭云)[a,b]‡

[a] State Key Laboratory of Magnetic Resonance and Atomic and Molecular Physics, Wuhan Institute of Physics and Mathematics, Chinese Academy of Sciences, Wuhan 430071, China

[b] Center for Cold Atom Physics, Chinese Academy of Sciences, Wuhan 430071, China

[c] Department of Physics, University of New Brunswick, Fredericton, New Brunswick, Canada E3B 5A3

(Received 16 November 2014; revised manuscript received 4 December 2014; published online 27 March 2015)

In this paper, we overview recent advances in high-precision structure calculations of the hydrogen molecular ions (H_2^+ and HD^+), including nonrelativistic energy eigenvalues and relativistic and quantum electrodynamic corrections. In combination with high-precision measurements, it is feasible to precisely determine a molecular-based value of the proton-to-electron mass ratio. An experimental scheme is presented for measuring the rovibrational transition frequency (v,L) : $(0,0) \to (6,1)$ in HD^+, which is currently underway at the Wuhan Institute of Physics and Mathematics.

Keywords: hydrogen molecular ion, rovibrational transition, proton-to-electron mass ratio, relativistic and QED corrections

PACS: 31.15.ac, 31.30.J–, 33.20.–t, 33.80.–b **DOI:** 10.1088/1674-1056/24/5/053102

1. Introduction

1.1. Proton-to-electron mass ratio m_p/m_e

Fundamental physical constants appear in mathematical formulas describing fundamental interactions in physical theories. Comparison of the same fundamental physical constant measured in different areas of physics can test the universality of the constant as well as the self-consistency of physical laws. The precision of a fundamental physical constant determines the accuracy of a theoretical prediction. Moreover, a space–time variation of a fundamental physical constant can reveal the domain of validity of a theory and provides further evidence for constructing a more general theory beyond the "standard model of particle physics".

The proton-to-electron mass ratio m_p/m_e is one of the fundamental physical constants, which is relevant to the quantum chromodynamic scale.[1] Its high precision value is of great importance for testing the standard model of particle physics, and for exploring new physics beyond the standard model.[2–5] Currently, the Committee on Data for Science and Technology (CODATA) recommended value for m_p/m_e is 1836.15267245 with the relative standard uncertainty of 4.1×10^{-10}.[6] This value is determined indirectly by measuring the masses of the proton and the electron separately. Since the relative uncertainties of m_p and m_e in the unified atomic mass unit (u) are 8.9×10^{-11} and 4.0×10^{-10} [6] respectively, the uncertainty in m_p/m_e is mainly due to the uncertainty of the electron mass. In fact, direct experimental measurement of m_e is challenging. One way to extract the electron mass is to compare the experimentally measured g factor of the electron in a hydrogenlike ion with the corresponding theoretical calculation based on quantum electrodynamic (QED) theory. This approach has been the most accurate method in the last decade.[7] Recently, Max Planck Institute for Nuclear Physics[8] in Germany has made a breakthrough on measuring the g factor of the electron in the hydrogenlike $^{12}C^{5+}$ and has determined the electron mass with the relative precision of 3×10^{-11}, a factor of 13 improvement over the CODATA recommended value.

In addition to indirect measurements, the proton-to-electron mass ratio can also be measured directly. Figure 1 shows the precision of m_p/m_e measured directly over the past 40 years. In earlier times, m_p/m_e was determined by measuring the cyclotron frequencies of a free proton and a free electron in the same magnetic field,[9–16] where the energy scales involved were in the high energy range of GeV to TeV. In the last decade, due to rapid development of new techniques, such as femtosecond optical comb and laser cooling and trapping, atomic and molecular spectroscopy can be measured to an unprecedented high precision at the level of Hz or sub-Hz, which has created many opportunities to test physical laws in low energy eV region.[17,18] With an increase of precision, small shifts in atomic and molecular energy levels can reveal small but subtle physical effects, such as high-order relativistic and QED (radiative) corrections, contributions from un-

*Project supported by the National Natural Science Foundation of China (Grants Nos. 11474316, 11004221, 10974224, and 11274348), the "Hundred Talent Program" of Chinese Academy of Sciences. Yan Zong-Chao was supported by NSERC, SHARCnet, ACEnet of Canada, and the CAS/SAFEA International Partnership Program for Creative Research Teams.

†Corresponding author. E-mail: zyan@unb.ca

‡Corresponding author. E-mail: tyshi@wipm.ac.cn

© 2015 Chinese Physical Society and IOP Publishing Ltd

known particles beyond the standard model of particle physics, and effects due to symmetry breakings.[19,20] A comparison between spectroscopic measurements and theoretical calculations can be used to determine fundamental physical constants involved, such as the proton-to-electron mass ratio m_p/m_e (or $m_{\bar{p}}/m_e$)[21–23] (see the last three measurements in Fig. 1). Direct and indirect measurements of m_p/m_e can not only provide diversified methods but also check self-consistency among the proton mass m_p, the electron mass m_e, and the ratio m_p/m_e. The self-consistency can ensure that these three constants are fundamental; furthermore a precise mass ratio m_p/m_e can impose a strict constraint on the individual values of m_p and m_e. A violation of this self-consistency may indicate the existence of new physics.

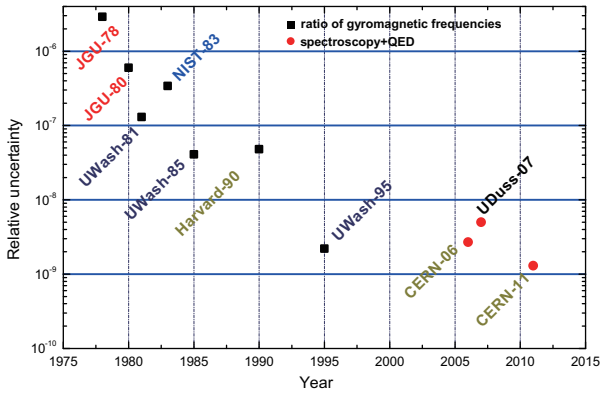


Fig. 1. Relative uncertainty of m_p/m_e measured directly. These measurements were carried out at Johannes Gutenberg-Universität Mainz (JGU),[9,10] University of Washington (UWash),[11–13] National Institute of Standards and Technology (NIST),[14] Harvard University (Harvard),[16] the European Organization for Nuclear Research (CERN),[21,22] and Heinrich-Heine-Universität Düsseldorf (UDuss).[23]

So far, several experiments have been performed to measure m_p/m_e (or $m_{\bar{p}}/m_e$) directly by studying spectroscopic data. These high precision measurements focus on the antiprotonic helium and the hydrogen molecular ions which can be used to directly determinate $m_{\bar{p}}/m_e$ and m_p/m_e, respectively. Moreover, a comparison between $m_{\bar{p}}/m_e$ and m_p/m_e can test the CPT (charge, parity, and time reversal) symmetry variation.

Since its establishment, the atomic spectroscopy and collisions using slow antiprotons (ASACUSA) collaboration has been working on precision spectroscopies of atoms containing the antiproton,[20] such as the antihydrogen atom ($\bar{H}$) and the antiprotonic helium atom ($\bar{p}He^+$), at the European organization for nuclear research (CERN). In 2006, ASACUSA measured 12 transition frequencies of the antiprotonic helium at the fractional precision of 9–16 ppb (1 ppb $\equiv 10^{-9}$), yielding the value of the antiproton-to-electron mass ratio $m_{\bar{p}}/m_e = 1836.152674(5)$,[21] in combination with the three-body QED calculations. In 2011, the two-photon spectroscopy of the antiprotonic helium containing 3 transition frequencies was reported with the achieved fractional precision of 2.3–5 ppb, which leads to the determination of $m_{\bar{p}}/m_e = 1836.1526736(23)$.[22] The $\bar{p}He^+$ atom can be generated by slowing down antiprotons in low temperature helium. Soon after its generation, the $\bar{p}He^+$ atom is then cooled to superfluid temperature $T \sim 1.5$ K for spectroscopic measurements within its short-lived 1-μs-scale lifetime (see Ref. [24] and references therein). Currently, the ASACUSA of CERN is the only group that is performing the measurements of $\bar{p}He^+$ transitional frequencies.

Compared to $\bar{p}He^+$, rovibrational states of hydrogen molecular ions (H_2^+ and HD^+) have longer lifetimes (ms to days) and can be sympathetically cooled to lower temperature of about 10 mK.[25] In 2007, Schiller and coworkers measured the transition frequency $(v,L) : (0,2) \to (4,3)$ in HD^+ to a relative precision of 2 ppb, which is consistent with the value of QED calculation to within 5 ppb.[23] In the above, v is the vibrational quantum number and L is the rotational quantum number. Later, they measured another HD^+ transition frequency $(v,L) : (0,0) \to (1,1)$ with a relative uncertainty being 1.1 ppb.[26] It should be pointed out that the theoretical calculations of the hydrogen molecular ions and the antiprotonic helium used in the above determinations are mainly due to the work by Korobov.[28–32] Although at this moment the direct determination of m_p/m_e is expected to be still less precise than the indirect determination, it will provide an important reference to the corresponding CODATA recommended value.

This article is organized as follows. The background of high-precision spectroscopy is introduced in Section 1.2 for hydrogen molecular ions, which includes theory and experiment. In Section 2, theoretical formulation for solving a three-body bound-state problem is presented, including the non-relativistic energy eigenvalue problem and the leading- and higher-order relativistic and QED corrections. In Section 3, an experimental scheme is described for measuring the rovibrational transition frequency $v : 0 \to 6$ in HD^+, which is currently underway at the Wuhan Institute of Physics and Mathematics. In Section 4, a summary is given.

1.2. Spectroscopies of hydrogen molecular ions

1.2.1. Theory

The hydrogen molecular ion, the simplest molecule in nature, can be considered as a three-body quantum mechanical system consisting of one electron and two nuclei. Some of its rovibrational states have lifetimes longer than 10 μs, and the probability of making a dipole transition can be strong enough to allow for a precision measurement of its spectroscopy.[2,27,33–35] On the other hand, the transition frequency between two specific rovibrational states can be calculated to sufficiently high precision using the three-body QED

theory.[30,31] Since the theoretical frequency of a rovibrational transition in the hydrogen molecular ion contains effects due to the proton-to-electron mass ratio, a comparison between theory and experiment of its spectroscopy holds a potential of extracting a precise value of m_p/m_e.[2,3]

Theoretically, a transition frequency in the hydrogen molecular ion can be expanded in powers of the fine structure constant α ($\approx 1/137$) according to the theory of nonrelativistic QED (NRQED).[36,37] The structure of an energy level contains the contributions from the nonrelativistic term, the leading-order relativistic and QED corrections of order $R_\infty\alpha^2$ and $R_\infty\alpha^3$ respectively, where R_∞ is the Rydberg constant, and the correction due to the finite nuclear size. Higher-order relativistic and QED corrections can be added in when they become necessary.

In order to determine a transition frequency, the nonrelativistic energy eigenfunction and the eigenvalue can be obtained by solving the three-body Schrödinger equation variationally. In previous work, the rovibrational states of the hydrogen molecular ions were calculated at different levels of approximation, such as the Born–Oppenheimer approximation, the adiabatic approximation, and the non-adiabatic approximation.[38–40] In 1985, Bishop and Solunac[41,42] broke down the Born–Oppenheimer and adiabatic approximation and calculated the energy levels of the hydrogen molecular ions precisely. From then on, the energy levels of H_2^+ and its isotopes have been evaluated to a precision of 10^{-15} [43–55] for most of the rovibrational states and of 10^{-30} or even better[56,57] for some low-lying states. One then needs to compute the relativistic and QED corrections to a sufficiently high order so that a meaningful comparison can be made with measured transition frequencies and hyperfine splittings. Figure 2 shows the time evolution of some theoretical transition frequencies and hyperfine splittings. To our knowledge, the hyperfine interaction between the electronic spin and nuclear spin in the hydrogen molecular ions was first calculated by Stephen and Auffray[58] in 1959. Soon after that, Dalgarno and coworkers[59] further calculated the electron spin–orbit and spin–spin interactions. From then on, many works were published on the calculation of the hyperfine interaction by means of the adiabatic approximation.[60–63] In 1991, the non-adiabatic corrections to the spin–spin interaction was computed by Babb and Dalgarno.[64] They also evaluated the non-adiabatic corrections to the electron spin–orbit interaction[65] and to the nuclear spin–rotation interaction.[66] In 2006, a calculation beyond the adiabatic approximation was performed by Korobov and coworkers[67] on the hyperfine structure in H_2^+. Since then, a series of work has been carried out to investigate the hyperfine structure of H_2^+,[68] HD^+,[69] HT^+,[70] and D_2^+.[71] It should be pointed out that these calculations on hyperfine structure were done in the frame of the Breit–Pauli Hamiltonian, which is accurate only to the order of $R_\infty\alpha^2$.[67] In 2009, the higher-order relativistic correction of $R_\infty\alpha^4(m_e/m_{nuc})$ to the hyperfine structure of H_2^+ was studied by Korobov *et al.*[72] For rovibrational transitions in the hydrogen molecular ions, early work on evaluating the relativistic and radiative corrections was performed in the framework of the Born–Oppenheimer approximation. To the best of our knowledge, the leading-order relativistic and radiative corrections of the hydrogen molecular ions were first calculated by Luke and coworkers[73] and by Gersten.[74] Since then, the rovibrational transition frequencies in the hydrogen molecular ions were systematically studied for low-lying states,[75] for all vibrational states with the rotational quantum number $L \leq 5$,[76,77] and for higher rotational states.[78] It should be mentioned that only the leading-order relativistic and radiative corrections had been studied before the Born–Oppenheimer approximation was lifted.

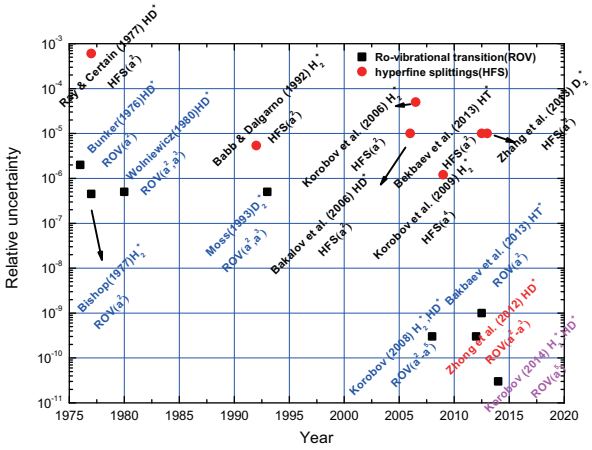


Fig. 2. Theoretical hyperfine splittings and rovibrational transition frequencies for the hydrogen molecular ions.

In 2006, Korobov[30] not only evaluated the $R_\infty\alpha^2$ and $R_\infty\alpha^3$ order corrections to high precision but also considered for the first time the higher-order terms of $R_\infty\alpha^4$ and $R_\infty\alpha^5$, beyond the adiabatic approximation. The largest part of the uncertainty in his calculation was due to the theoretical approximation of the $R_\infty\alpha^5$ term. The uncertainty in the transition frequency $(v,L):(0,0)\rightarrow(1,0)$ for H_2^+ was thus estimated to be about 0.08 MHz, at the level of 1 ppb. Soon after that, an improved calculation for the second-order and the $R_\infty\alpha^5$ terms was performed,[31] which reduced the total uncertainty in the transition frequency of $(v,L):(0,0)\rightarrow(1,0)$ to 25 kHz at 0.3 ppb. The leading-order relativistic corrections of some important transitions in H_2^+ and HD^+ were independently verified by Zhong *et al.*,[79,80] where the computational uncertainties were completely eliminated and the remaining uncertainties were entirely due to the uncertainties in the fundamental physical constants used. In 2012, the uncertainties of the leading-order radiative corrections were reduced, respectively, from 2 kHz to 4 Hz and 40 Hz for the transition (v,L) :

$(0,0) \to (1,0)$ in H_2^+ and HD^+.[81] Recently, Korobov and coworkers developed a method for calculating the relativistic Bethe logarithmic term for a general two-center problem.[82] Very recently they completed a calculation for the $R_\infty\alpha^5$ order radiative corrections for H_2^+, HD^+, and the antiprotonic helium.[83,84] Therefore, the total uncertainty has now been reduced to 2 kHz for the transition $(v,L) : (0,0) \to (1,0)$ in H_2^+ and HD^+. In other words, the relative uncertainty of theoretical spectroscopy is reduced to about 0.03 ppb. Thus if the experimental uncertainty can reach the level of 0.2 ppb, then the proton-to-electron mass ratio can be determined at the level of 0.5 ppb.

1.2.2. Experiment

Spectroscopic measurements of rovibrational and hyperfine structures of hydrogen molecular ions have been carried out since 1960s. Figure 3 shows a time evolution of some important measurements. During the early stages, the measured spectra were much less precise than their neutral counterparts. High-order relativistic and QED effects of spin–spin and spin–orbital interactions have never been tested on these ions until recently. With developments of new experimental techniques, such as laser cooling and trapping, and sympathetic cooling,[85] together with the emergence of new laser systems,[86] precision measurements of cold molecules and molecular ions have received considerable attention. Cold and trapped ions have a range of advantages for spectroscopic applications. First, experiment on single trapped ions can avoid inhomogeneous spectral line broadening resulting from ensemble averaging. Second, the low translational velocities of the ions can minimize Doppler broadening. Third, a long storage time allows a measurement to go over an extended period of time. Finally, an ultra-high vacuum apparatus provides a well-defined experimental environment where interactions with surroundings are minimized or well controlled. All these can make enhancement of spectroscopic resolution possible.

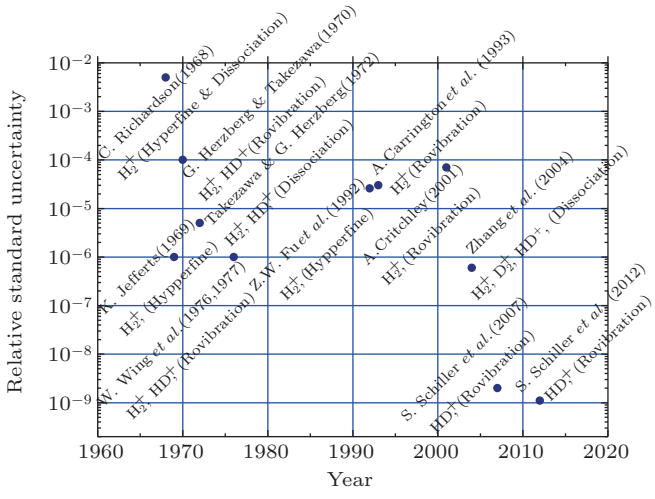


Fig. 3. Relative uncertainties of various spectroscopies of the hydrogen molecular ions.

Schiller's group at Düsseldorf[23,33] pioneered an experimental measurement of a rovibrational transition in sympathetically cooled HD^+ ions. In their experiments, the HD^+ ions were sympathetically cooled into a Be^+ Coulomb crystal. High-resolution infrared spectroscopy on the HD^+ ions was recorded for the rovibrational transition of $(v,L) : (0,2) \to (4,3)$ at a wavelength around 1.4 μm. Though the spectral resolution of about 40 MHz was limited by the residual Doppler broadening, the spectral line position was determined with a relative accuracy of 2 ppb. Combining with the Korobov's theoretical prediction, the proton-to-electron mass ratio m_p/m_e was determined at the level of 5 ppb. In 2012, the same group made further progress on the measurement of the rovibrational transition $(v,L) : (0,0) \to (1,1)$ with the accuracy of 1.1 ppb.[26] The improvement of the experimental accuracy was achieved by using the optical pumping method to increase the rovibrational ground state population. The population transfer efficiency was achieved at 60%–70% in their experiments.[87] There are other two groups currently working on the precision spectroscopy of the hydrogen molecular ions HD^+ and H_2^+. The experiment with a goal of 5×10^{-9} accuracy is currently set up at University of Amsterdam by measuring the $v : 0 \to 8$ transition on the cold HD^+ ions.[27] Although high quantum overtone transitions are very weak, using a high power laser system they were able to observe a promising signal. Meanwhile, the group led by Hilico at Laboratoire Kastler Brossel in Paris has devoted to measuring the two-photon transition $(v,L) : (0,0) \to (1,0)$ in H_2^+ aiming at the accuracy of 0.1 ppb.[88]

2. Theoretical calculations of H_2^+ and HD^+

According to the theory of NRQED,[36,37] the total energy of a state in H_2^+ or HD^+ can be expressed in powers of the fine structure constant α

$$E_{\rm total} = E_{\rm nr} + E_{\rm nuc} + E_{\rm hfs} + E^{(2)} + E^{(3)} + E^{(4)} + E^{(5)} + O(\alpha^6), \quad (1)$$

where $E_{\rm nr}$ is the nonrelativistic energy, $E_{\rm nuc}$ is the correction due to the finite nuclear size, $E_{\rm hfs}$ is the correction from the hyperfine structure, and $E^{(n)}$ is the correction of order $R_\infty\alpha^n$. The effect of hyperfine structure in an experimental measurement can be removed according to theoretical calculation of hyperfine splittings, and the transitional frequency is then obtained. $E_{\rm hfs}$ has been well calculated in series of works for HD^+[69] and H_2^+[67,68,72,79] and thus its calculations are not presented in this article. To determine the proton-to-electron mass ratio at the level of ppb or sub-ppb, we need to consider relativistic and radiative corrections up to order $R_\infty\alpha^5$, which can be evaluated perturbatively using nonrelativistic wavefunctions. In the following, atomic units are used where $m_e = e = \hbar = 1$, unless otherwise stated.

2.1. Nonrelativistic energy and wavefunction

We begin with the nonrelativistic Hamiltonian of a three-body Coulombic system,

$$H_0 = -\frac{1}{2m_0}\nabla_{R_0}^2 - \frac{1}{2m_1}\nabla_{R_1}^2 - \frac{1}{2m_2}\nabla_{R_2}^2 + \frac{q_0q_1}{|\boldsymbol{R}_0-\boldsymbol{R}_1|} + \frac{q_0q_2}{|\boldsymbol{R}_0-\boldsymbol{R}_2|} + \frac{q_1q_2}{|\boldsymbol{R}_1-\boldsymbol{R}_2|}, \quad (2)$$

where m_i, q_i, and $\boldsymbol{R}_i$ are the mass, charge, and position vector of the ith particle, respectively. The total angular momentum operator, which commutes with H_0, is

$$\boldsymbol{L} = -\mathrm{i}\boldsymbol{R}_0\times\nabla_{R_0} - \mathrm{i}\boldsymbol{R}_1\times\nabla_{R_1} - \mathrm{i}\boldsymbol{R}_2\times\nabla_{R_2}. \quad (3)$$

For the purpose of isolating the center-of-mass motion, we make the following coordinate transformations:

$$\boldsymbol{r}_1 = \boldsymbol{R}_1 - \boldsymbol{R}_0, \quad \boldsymbol{r}_2 = \boldsymbol{R}_2 - \boldsymbol{R}_0,$$
$$\boldsymbol{X} = \frac{1}{M}(m_0\boldsymbol{R}_0 + m_1\boldsymbol{R}_1 + m_2\boldsymbol{R}_2), \quad (4)$$

where $M = \sum_{i=0}^{2} m_i$ is the total mass of the system and $\boldsymbol{X}$ is the position vector of the center of mass of the system. In terms of the new coordinates $\boldsymbol{r}_1$, $\boldsymbol{r}_2$, and $\boldsymbol{X}$, H_0 and $\boldsymbol{L}$ can be written in the form of

$$H_0 = -\frac{1}{2\mu_1}\nabla_{r_1}^2 - \frac{1}{2\mu_2}\nabla_{r_2}^2 - \frac{1}{2M}\nabla_X^2 - \frac{1}{m_0}\nabla_{r_1}\cdot\nabla_{r_2} + \frac{q_0q_1}{r_1} + \frac{q_0q_2}{r_2} + \frac{q_1q_2}{r_{12}}, \quad (5)$$

$$\boldsymbol{L} = -\mathrm{i}\boldsymbol{X}\times\nabla_X - \mathrm{i}\boldsymbol{r}_1\times\nabla_{r_1} - \mathrm{i}\boldsymbol{r}_2\times\nabla_{r_2}, \quad (6)$$

where $r_{12} = |\boldsymbol{r}_1 - \boldsymbol{r}_2|$ and $\mu_i = m_i m_0/(m_i+m_0)$. Since $\boldsymbol{X}$ is cyclic, we can simply neglect $\boldsymbol{X}$. Therefore in the center-of-mass frame,

$$H_0 = -\frac{1}{2\mu_1}\nabla_{r_1}^2 - \frac{1}{2\mu_2}\nabla_{r_2}^2 - \frac{1}{m_0}\nabla_{r_1}\cdot\nabla_{r_2} + \frac{q_0q_1}{r_1} + \frac{q_0q_2}{r_2} + \frac{q_1q_2}{r_{12}}, \quad (7)$$

$$\boldsymbol{L} = -\mathrm{i}\boldsymbol{r}_1\times\nabla_{r_1} - \mathrm{i}\boldsymbol{r}_2\times\nabla_{r_2}. \quad (8)$$

This Hamiltonian can be thought of as the one describing two "effective particles" moving relative to particle 0 sitting at the origin. It is noted that one has freedom to choose any particle as particle 0. For the hydrogen molecular ions H_2^+ and HD^+, we choose the nucleus of larger mass as particle 0, the electron as particle 1, and the other nucleus as particle 2.

The Schrödinger equation for the system is therefore expressed as $H_0\psi_0 = E_0\psi_0$, where E_0 is the energy eigenvalue and ψ_0 is the corresponding eigenfunction. For solving the eigenvalue problem for H_0 variationally, we seek the common eigenstates of the commuting observables $\{H_0, \boldsymbol{L}^2, L_z, \Pi\}$, where Π is the parity operator, using the following basis set in Hylleraas coordinates:

$$\phi_{ijk}(\boldsymbol{r}_1,\boldsymbol{r}_2) = r_1^{l_1+i} r_2^{j_0+j} r_{12}^k \,\mathrm{e}^{-\alpha r_1-\beta r_2}\mathcal{Y}_{LM_L}^{l_1l_2}(\boldsymbol{r}_1,\boldsymbol{r}_2). \quad (9)$$

In the above, $\mathcal{Y}_{LM_L}^{l_1l_2}(\boldsymbol{r}_1,\boldsymbol{r}_2)$ is the vector coupled product of spherical harmonics for particles 1 and 2 forming the common eigenstate of $\boldsymbol{L}^2$, L_z, and Π with the corresponding eigenvalues of $L(L+1)$, M_L, and $(-1)^{l_1+l_2}$, respectively

$$\mathcal{Y}_{LM_L}^{l_1l_2}(\boldsymbol{r}_1,\boldsymbol{r}_2) = \sum_{m_1m_2}\langle l_1l_2m_1m_2|LM_L\rangle \mathrm{Y}_{l_1m_1}(\boldsymbol{r}_1)\mathrm{Y}_{l_2m_2}(\boldsymbol{r}_2). \quad (10)$$

The vibrational degrees of freedom between two the nuclei should be sufficiently represented in the basis set, according to the picture of the Born–Oppenheimer approximation, as pointed out by Bhatia and Drachman.[89] They suggested to use Gaussian-like function $\rho^N \mathrm{e}^{-b\rho}$ to simulate the vibrational modes, where ρ is the distance between the two nuclei, and N and b are two big numbers satisfying $b \approx N/2$. Since we choose one nucleus as particle 0 and the other as particle 2, the vibrational part in our basis can be described by $r_2^{j_0+j}\mathrm{e}^{-\beta r_2}$. For low rovibrational states, the lowest power of r_2 is set to be $j_0 = 35$ and 45 for H_2^+ and HD^+, respectively. Also i, j, and k in Eq. (9) are non-negative integers. Furthermore, the nonlinear parameters are initially chosen to be $\alpha \approx 1$ and $\beta \approx 15$–20.

If the two nuclei are identical, such as H_2^+, the symmetry is preserved in the Hamiltonian for the permutation of the two nuclei. We can thus choose a basis which has the permutational symmetry explicitly adapted. On the other hand, we are also free to choose a basis by not explicitly imposing the permutational symmetry.[53] We denote the permutation operation between the two identical nuclei by P_{nuc}, which implies that the eigenvalues of P_{nuc} are $(-1)^{S_{\mathrm{p}}}$ with $S_{\mathrm{p}} = 0, 1$, corresponding to the singlet and triplet states, respectively. Furthermore, $\boldsymbol{L}$ is also invariant under P_{nuc}. It is thus possible to find the common eigenstates for the commuting observables $\{H_0, \boldsymbol{L}^2, L_z, \Pi, P_{\mathrm{nuc}}\}$. For a given total angular momentum L, for a state of natural parity, the independent angular configurations (l_1, l_2) in a wavefunction are those satisfying the condition $l_1 + l_2 = L$

$$(0,L),(1,L-1),\ldots,(L,0). \quad (11)$$

Each configuration (l_1, l_2) has its own nonlinear parameters α and β. Since the nuclei carry most of the angular momentum, the leading configuration $(0, L)$ is divided into N_L sub-blocks, each having its own nonlinear parameters α and β, according to the following scheme:[53] the nth block in the configuration $(0, L)$ contains all the terms satisfying the following relations for the power j_n of r_2:

$$g_n < j_n \le g_{n+1}, \quad n = 1,2,\ldots,N_L, \quad (12)$$

where

$$g_n = \mathrm{int}\left[\frac{\Omega}{N_L}(n-1)\right], \quad (13)$$

int[x] stands for the integer part of x, and Ω is an integer controlling the size of each block. The basis set is generated by including all terms such that

$$i+j+k \le \Omega. \tag{14}$$

The basis set constructed this way can sufficiently represent the vibrational modes in the wavefunction. Moreover, if we include some terms with lower powers of r_2, the rate of convergence, along with the numerical stability in the wavefunction, can be further enhanced.[56] Hence another small-size block with $j_0 = l_2$ is added to our basis set. A complete optimization is performed with respect to those nonlinear parameters by minimizing the energy eigenvalue. This involves the calculation of the energy derivative $\partial E/\partial\alpha$ with respect to each nonlinear parameters.[55]

The basic type of integrals that appear in our variational calculation are of the form

$$I(a,b,c;\alpha,\beta) = \int \mathrm{d}\boldsymbol{r}_1\,\mathrm{d}\boldsymbol{r}_2 \mathcal{Y}^{l_1' l_2'}_{L' M_L'}(\boldsymbol{r}_1,\boldsymbol{r}_2)^* \times \mathcal{Y}^{l_1 l_2}_{L M_L}(\boldsymbol{r}_1,\boldsymbol{r}_2)\, r_1^a r_2^b r_{12}^c\, \mathrm{e}^{-\alpha r_1 - \beta r_2}, \tag{15}$$

which can be evaluated analytically in terms of the hypergeometric function ${}_2\mathrm{F}_1(a,b;c;x)$.[90] The procedure for handling singular integrals appearing in the evaluation of the Breit operators can be found in Ref. [91] where the singular parts are exactly canceled out with each other. Another method to deal with singular integrals was developed by Harris and coworkers[92] where the singular parts are simply dropped out. It should be pointed out that these two methods are equivalent.

Table 1. Nonrelativistic energies for various rovibrational states in H_2^+ and HD^+. The mass ratios of $m_p/m_e = 1836.15267245$ and $m_d/m_e = 3670.4829652$ are taken from the 2010 CODATA set.[6]

(v,L)	H_2^+	HD^+
(0,0)	–0.597139063079144251108031025395(3)	–0.597897968608892577899511752764(6)
(0,1)	–0.596873738784442268913358 30(3)	–0.597698128192059568078743 05(7)
(0,2)	–0.596345205489075284602037 3(2)	–0.597299643351606083357910(2)
(0,3)	–0.595557638979926416186902(4)	–0.596704882761683549294 01(3)
(0,4)	–0.594517169238493025363 7(2)	–0.595917342212554048695 7(3)
(1,0)	–0.587155679095532687829019 4007(1)	–0.589181829556578469182321 4177(4)
(1,1)	–0.586904320918513700711 4739(5)	–0.588991111991646700668530(2)
(1,2)	–0.586403631527974188229395(6)	–0.588610829389373517138 82(3)
(1,3)	–0.585657611876878197786 2(2)	–0.588043264162391979393 3(4)
(1,4)	–0.584672134228050303 04(6)	–0.587291784373731521 51(3)
(2,0)	–0.577751904414067229657555467(2)	–0.580903700217773751175193655(2)
(2,1)	–0.577514034056410935795 82(1)	–0.580721828120326552940 8(2)
(2,2)	–0.577040237161949676202 8(3)	–0.580359195199257017786 5(6)
(2,3)	–0.576334350218495570 18(6)	–0.579818002027213799 83(2)
(2,4)	–0.575402003297637141 2(2)	–0.57910149556479679 25(2)
(3,0)	–0.568908498729535152478035082(7)	–0.573050546551079311929890 8(2)
(3,1)	–0.568683708258842165049(1)	–0.572877277093417222702(2)
(3,2)	–0.568235992970197563839(7)	–0.572531810325156663 22(5)
(3,3)	–0.567569034832072494(5)	–0.57201626923167226 61(2)
(3,4)	–0.566688236628213 25(2)	–0.57133378604512134(2)
(4,0)	–0.560609220848067959063757 5(2)	–0.565611042075852914783012(1)
(4,1)	–0.560397171398673979 30(2)	–0.565446166276609180 7(2)
(4,2)	–0.559974864818409748 52(5)	–0.565117449762754388 1(5)
(4,3)	–0.559345838226583 60(2)	–0.564626942061051144(2)
(4,4)	–0.55851528162414 81(3)	–0.563977666866578 9(5)

The nonrelativistic energies of the hydrogen molecular ions H_2^+ and HD^+ for various rovibrational states, together with the corresponding uncertainties, are presented in Table 1. The energy eigenvalues are converged to about 30 significant digits for the ground states of H_2^+ and HD^+. For excited rovibrational states, however, we can still obtain at least 16 significant digits, which is sufficient for our calculations of relativistic and radiative corrections.

2.2. Leading-order relativistic corrections

The leading-order relativistic corrections due to the Breit operators are $R_\infty\alpha^2$. For a general atomic or molecular system, these corrections can be obtained by reducing the relativistic four-component wavefunction of the Dirac equation to a two-component one in its nonrelativistic form.[93–96] The major part of the $R_\infty\alpha^2$ corrections is due to the relativistic bound electron which, for the hydrogen molecular ion, has the form of

$$E^{(2)}_{\mathrm{rc}} = \alpha^2 \left\{ -\frac{1}{8}\langle \nabla^4_{r_1} \rangle + \frac{\pi}{2}[\langle \delta(\boldsymbol{r}_1)\rangle + \langle \delta(\boldsymbol{r}_{12})\rangle] \right\}. \tag{16}$$

There also exist the so-called recoil corrections of $R_\infty\alpha^2(m_e/m_{\mathrm{nuc}})$ and $R_\infty\alpha^2(m_e/m_{\mathrm{nuc}})^2$, which are caused by the finite nuclear masses. The first of this type is the retardation terms coming from the exchange of transverse photon

$$E^{(2)}_{\mathrm{ret}} = \alpha^2 \sum_{i<j} q_i q_j R_{ij}, \quad i,j = 0,1,2, \tag{17}$$

where

$$R_{01} = -\frac{1}{2m_0m_1}\left\langle \frac{\nabla_{r_1}\cdot(\nabla_{r_1}+\nabla_{r_2})}{r_1} + \frac{r_1r_1:(\nabla_{r_1}+\nabla_{r_2})\nabla_{r_1}}{r_1^3}\right\rangle, \quad (18)$$

$$R_{02} = -\frac{1}{2m_0m_2}\left\langle \frac{\nabla_{r_2}\cdot(\nabla_{r_1}+\nabla_{r_2})}{r_2} + \frac{r_2r_2:(\nabla_{r_1}+\nabla_{r_2})\nabla_{r_2}}{r_2^3}\right\rangle, \quad (19)$$

$$R_{12} = \frac{1}{2m_1m_2}\left\langle \frac{\nabla_{r_1}\cdot\nabla_{r_2}}{r_{12}} + \frac{r_{12}r_{12}:\nabla_{r_1}\nabla_{r_2}}{r_{12}^3}\right\rangle. \quad (20)$$

The correction $E_{\rm ret}^{(2)}$ can be understood as the interaction between the magnetic dipole moments of the particles involved, arising from the orbital motion of the charges (also called the orbit–orbit interaction). The next part is the relativistic kinetic energy correction for the two nuclei

$$E_{\rm kin}^{(2)} = -\alpha^2\left\{\frac{\langle(\nabla_{r_1}+\nabla_{r_2})^4\rangle}{8m_0^3} + \frac{\langle\nabla_{r_2}^4\rangle}{8m_2^3}\right\}, \quad (21)$$

which is rooted from the dependence of the relativistic mass on velocity: $E_{\rm kin} = \sqrt{m^2+p^2} \approx m + p^2/(2m) - p^4/(8m^3)\cdots$. Furthermore, there is the so-called Darwin term that arises from the nuclear spin-dependent recoil correction for a particle of spin-$\frac{1}{2}$, such as the proton. The Darwin term vanishes for the case of spin-0 or spin-1 nucleus, such as the ^{4}He nucleus or the deuteron.[97] Therefore, the Darwin term for H_2^+ is

$$E_{\rm Darwin}^{(2)} = \alpha^2\frac{\pi}{2}\left\{\frac{\langle\delta(r_1)\rangle}{m_0^2} + \frac{\langle\delta(r_{12})\rangle}{m_2^2}\right\}, \quad (22)$$

and the Darwin term for HD^+ is

$$E_{\rm Darwin}^{(2)} = \alpha^2\frac{\pi}{2}\frac{\langle\delta(r_{12})\rangle}{m_2^2}. \quad (23)$$

The complete contribution of the leading-order relativistic correction is thus

$$E^{(2)} = E_{\rm rc}^{(2)} + E_{\rm ret}^{(2)} + E_{\rm kin}^{(2)} + E_{\rm Darwin}^{(2)}. \quad (24)$$

For the case of H_2^+, the permutation symmetry of the two protons implies that

$$\langle\delta(r_1)\rangle = \langle\delta(r_{12})\rangle,$$
$$R_{01} = R_{12}, \quad \langle(\nabla_{r_1}+\nabla_{r_2})^4\rangle = \langle\nabla_{r_2}^4\rangle. \quad (25)$$

The numerical values for the above discussed operators are presented in Table 2 for H_2^+ and in Table 3 and Table 4 for HD^+.

Table 2. Numerical values of the Breit operators $\langle\delta(r_1)\rangle$, $\langle\nabla_{r_1}^4\rangle$, $\langle\nabla_{r_2}^4\rangle$, R_{01}, and R_{02} for H_2^+, where $v = 0$–4 and $L = 0$–4.

(v,L)	$\langle\delta(r_1)\rangle$	$\langle\nabla_{r_1}^4\rangle$	$\langle\nabla_{r_2}^4\rangle$	R_{01}	R_{02}
(0,0)	0.2067364762886640 04(4)	6.2856600593074270(7)	79.79764930578(5)	1.170117625032930(1)	4.601934312292 76(3)
(0,1)	0.2064913201586455(1)	6.27803903738084(1)	85.0504556068(1)	1.168818663818102(7)	4.83433647345744(1)
(0,2)	0.2060045428253964 7(2)	6.26290995769249(3)	96.91090513728(1)	1.166239006846765 3(1)	5.293427387814051(1)
(0,3)	0.2052830770543 85(3)	6.240494331036(2)	117.976351526(8)	1.16241450178322(5)	5.96806152239636(1)
(0,4)	0.2043369902118 21(1)	6.21111373390(1)	151.874397816(6)	1.15739726546214(3)	6.842198148013057 1(2)
(1,0)	0.2013106647017149(4)	6.12451980773668(3)	334.89830189(5)	1.14080522712808(8)	12.89614649422(1)
(1,1)	0.201081173073537(2)	6.11739730750(2)	347.54872540(2)	1.139597149439(4)	13.0952920268(3)
(1,2)	0.200625548551648(1)	6.10325962914552(6)	373.997618687(2)	1.137198302449808(6)	13.488286549835(3)
(1,3)	0.19995037648835(4)	6.0823171614(3)	416.4349042(3)	1.13364264773 95(5)	14.06480755353873(5)
(1,4)	0.19906521542714(5)	6.05487519861(4)	477.89237015(7)	1.1289795422565(4)	14.810022086899788(2)
(2,0)	0.1962945882927300(1)	5.976228559885276(9)	762.803695574(1)	1.114077225483 36(1)	19.878981012746(1)
(2,1)	0.196079942033917(5)	5.9695793169698(7)	780.9216157(2)	1.112955681491(6)	20.0477078807(2)
(2,2)	0.1956538427886285(7)	5.956382859214(3)	818.12463906(1)	1.1107290113251(1)	20.380248727985(3)
(2,3)	0.19502254990888(7)	5.9368391478(2)	876.2466269(3)	1.107429422937(1)	20.867037676117 87(1)
(2,4)	0.1941951450844(1)	5.9112382321(2)	957.7993482(5)	1.103103710671(6)	21.494350160804(2)
(3,0)	0.1916624972506 60(4)	5.8400118488205(1)	1304.20928519(5)	1.089801608607 71(4)	25.661621333295(5)
(3,1)	0.1914619817000 93(3)	5.8338140022328(6)	1326.12198978(1)	1.088762925947 33(1)	25.802345688983(3)
(3,2)	0.1910639883251 1(1)	5.821515365437(5)	1370.7553662(2)	1.086701150024(5)	26.079235660105(5)
(3,3)	0.1904744702670(2)	5.803306116(3)	1439.630107(2)	1.083646859106(4)	26.483422979178(8)
(3,4)	0.1897020619107(7)	5.7794620161(6)	1534.8012755(8)	1.079644469587(5)	27.002203039973(3)
(4,0)	0.1873918466646(3)	5.71519849517(8)	1908.37170(2)	1.0678682734(1)	30.33829428(1)
(4,1)	0.187204844125(2)	5.70943335888(2)	1932.6198429(5)	1.0669094254(3)	30.45305164(3)
(4,2)	0.1868337304667(1)	5.697995472387(8)	1981.782888(1)	1.065006550320(2)	30.678335448958(8)
(4,3)	0.1862841710550(7)	5.681065831(1)	2057.103974(2)	1.06218871317(1)	31.0059220217(1)
(4,4)	0.1855643805 19(5)	5.65890681(2)	2160.234041(5)	1.0584981285(1)	31.424047350261(4)

Table 3. Numerical values of the Breit operators $\langle\delta(\boldsymbol{r}_{12})\rangle$, $\langle\delta(\boldsymbol{r}_1)\rangle$, $\langle\boldsymbol{\nabla}^4_{r_1}\rangle$, $\langle\boldsymbol{\nabla}^4_{r_2}\rangle$, and $\langle(\boldsymbol{\nabla}_{r_1}+\boldsymbol{\nabla}_{r_2})^4\rangle$ for HD^+, where $v = 0$–4 and $L = 0$–4.

(v,L)	$\langle\delta(\boldsymbol{r}_{12})\rangle$	$\langle\delta(\boldsymbol{r}_1)\rangle$	$\langle\boldsymbol{\nabla}^4_{r_1}\rangle$	$\langle\boldsymbol{\nabla}^4_{r_2}\rangle$	$\langle(\boldsymbol{\nabla}_{r_1}+\boldsymbol{\nabla}_{r_2})^4\rangle$
(0,0)	0.20704259947747190 04(2)	0.20734814178029706 66(2)	6.3001999476785933(6)	104.371713686093(1)	104.443848901053(2)
(0,1)	0.206857699572752 56(1)	0.207163241677423572(7)	6.294450746055923(5)	110.38493981778(2)	110.4613313632(1)
(0,2)	0.20648990097608551(7)	0.2067954443349440(4)	6.2830163299151(5)	123.79001412764(6)	123.8756587418(6)
(0,3)	0.20594314768281(1)	0.2062486970164612(4)	6.266022789768(7)	147.25876381(2)	147.36009295(4)
(0,4)	0.20522321312906(3)	0.205528777980949(6)	6.24365466610(2)	184.59247475(2)	184.7179604(1)
(1,0)	0.20228886473978993(2)	0.20260117861162289(2)	6.15902235229201(4)	449.45675946471(2)	449.7391462670(1)
(1,1)	0.20211421220190804(1)	0.20242655716340313(3)	6.15359974575108(2)	464.36193814804(1)	464.6533872074(1)
(1,2)	0.2017668215015289(1)	0.2020792303568918(5)	6.142815739370(1)	495.3679016186(8)	495.678116390(6)
(1,3)	0.2012504647824(3)	0.2015629737358(2)	6.1267909226(3)	544.7845009(2)	545.1244240(5)
(1,4)	0.2005706622275(5)	0.20088331251301(2)	6.1057017310(3)	615.8801839(4)	616.262509(1)
(2,0)	0.19784583746893604(2)	0.19816679512560184 14(8)	6.02761432267228(1)	1042.81683129264(3)	1043.44331653088(5)
(2,1)	0.1976809559785677(9)	0.198001981206342(1)	6.0225036774882(2)	1064.624132727(1)	1065.263406622(4)
(2,2)	0.197353025118044(5)	0.1976741873189976(5)	6.012340962862(5)	1109.271531087(7)	1109.93693530(3)
(2,3)	0.19686565432911(8)	0.19718702654295(2)	5.9972415652(1)	1178.74702791(2)	1179.4529688(1)
(2,4)	0.1962241242204(1)	0.1965457848848(2)	5.97737426240(4)	1275.84569327(1)	1276.6080713(2)
(3,0)	0.1936960139249636(3)	0.1940278413804545(3)	5.90545343248 85(7)	1812.997565364(1)	1814.063236354(2)
(3,1)	0.1935404783766321(6)	0.193872416785920(1)	5.9006418093939(4)	1839.951687858(5)	1841.032921943(3)
(3,2)	0.193231161405204(1)	0.193563323743184(3)	5.89107464757(3)	1894.7472155(5)	1895.8600500(8)
(3,3)	0.192771518257(4)	0.19310402152252(7)	5.876862410(2)	1979.084658(2)	1980.246050(8)
(3,4)	0.19216660268 1(1)	0.192499569868(1)	5.8581666305(8)	2095.33663918(2)	2096.564775(2)
(4,0)	0.189823702852585(7)	0.19016909089076(3)	5.7920773795339(5)	2697.669274(1)	2699.2354157(9)
(4,1)	0.18967713560504(1)	0.1900226872284(1)	5.7875534285 65(6)	2728.2144158(1)	2729.7980517(2)
(4,2)	0.18938568121580(3)	0.18973156232654(8)	5.77855925079(2)	2790.0612310(3)	2791.6802590(4)
(4,3)	0.18895264869(6)	0.18929902980(2)	5.7652006889(6)	2884.65201(1)	2886.32533(6)
(4,4)	0.188382876738(6)	0.188729935330(3)	5.747632304(5)	3013.980528(6)	3015.72739(3)

Table 4. Numerical values of the Breit operators R_{02}, R_{01}, and R_{12} for HD^+, where $v = 0$–4 and $L = 0$–4.

(v,L)	R_{02}	R_{01}	R_{12}
(0,0)	5.35463051901711943(7)	1.174487825932605556(3)	1.170770145051139727(2)
(0,1)	5.589562255342723(1)	1.1735785001855910(1)	1.1697193799366195(4)
(0,2)	6.055104818249343733(4)	1.171769108405540(2)	1.16762928124835329(3)
(0,3)	6.74277630617217739(6)	1.16907791520748(2)	1.1645223841766(2)
(0,4)	7.640242669140628(6)	1.165531695329 56(5)	1.1604316913454(5)
(1,0)	15.14482588936280077(6)	1.1504812637673131(2)	1.1433664050045(2)
(1,1)	15.350575279863064(1)	1.1496258585220391(3)	1.142380739612368 55(7)
(1,2)	15.758027637524 10(4)	1.147923888699637(7)	1.140420315240445(2)
(1,3)	16.35924480624(3)	1.145392790044(2)	1.13750662824(1)
(1,4)	17.1426952788899(3)	1.1420581168039(4)	1.133671151272(3)
(2,0)	23.59899696623698(2)	1.1282362008927494(6)	1.1181235693136(2)
(2,1)	23.777762089355404(4)	1.1274325102467439(1)	1.117200151023 88(1)
(2,2)	24.13150123361982(4)	1.12583357622946(1)	1.115363727098 30(3)
(2,3)	24.6527816700128(9)	1.12345605684 68(8)	1.112634817630(2)
(2,4)	25.3308170266259(7)	1.120324362118(2)	1.109043458742(1)
(3,0)	30.817653008622(1)	1.10767720643593(3)	1.0949375427689(2)
(3,1)	30.97134959374(1)	1.1069233223353(1)	1.094073892137 15(9)
(3,2)	31.275189712792(3)	1.1054236322514(2)	1.0923565391832(2)
(3,3)	31.72221152212(6)	1.103194064780(2)	1.0898050864(1)
(3,4)	32.30232200847(1)	1.100257957806(8)	1.0864482210 81(5)
(4,0)	36.88807887511(1)	1.088739929649(8)	1.073718403917(3)
(4,1)	37.0183653341(6)	1.08803423109(2)	1.07291239499(1)
(4,2)	37.275607599566(2)	1.086630566009(1)	1.071309888849 88(7)
(4,3)	37.65328339(4)	1.0845441798(5)	1.068929626(1)
(4,4)	38.14194609(1)	1.0817974074(2)	1.0657990275(3)

2.3. Leading-order radiative corrections

The leading-order radiative corrections of $R_\infty\alpha^3$ is the largest part of the QED shift. For an atomic or molecular bound state, the current theoretical formalism for evaluating the QED corrections is based on the NRQED theory.[36,98–100] The one-loop self-energy correction is

$$E_{\rm se}^{(3)} = \frac{4\alpha^3}{3}\left(\ln\frac{1}{\alpha^2} - \beta(v,L) + \frac{5}{6} - \frac{3}{8}\right) \times [\langle\delta(\boldsymbol{r}_1)\rangle + \langle\delta(\boldsymbol{r}_{12})\rangle], \tag{26}$$

where $\beta(v,L)$ is the Bethe logarithm. The correction of the anomalous magnetic moment of order $R_\infty\alpha^3$ is

$$E_{\rm anom}^{(3)} = \frac{\alpha^3}{2}[\langle\delta(\boldsymbol{r}_1)\rangle + \langle\delta(\boldsymbol{r}_{12})\rangle], \tag{27}$$

which may be integrated into Eq. (26) as a contribution from the form factor of the electron.[101] The Coulomb interaction between the bound electron and an external field can be represented by exchanging Coulomb photons. According to QED, a Coulomb photon generates virtual electron–positron pairs which are then annihilated into photons. As a result, the energy of the Coulomb photon has a shift. The correction of one-loop vacuum polarization, which has one electron–positron pair, is

$$E_{\rm vp}^{(3)} = \frac{4\alpha^3}{3}\left(-\frac{1}{5}\right)[\langle\delta(\boldsymbol{r}_1)\rangle + \langle\delta(\boldsymbol{r}_{12})\rangle]. \tag{28}$$

The interaction that the bound electron exchanges a Coulomb photon and a transverse photon with nucleus contributes to the energy shift. Thus, the order $R_\infty\alpha^3(m_{\rm e}/m_{\rm nuc})$ correction of one transverse photon exchange is

$$E_{\rm tr-ph}^{(3)} = \alpha^3\left\{\frac{2}{3}\left[-\ln\alpha - 4\beta(v,L) + \frac{31}{3}\right] \times \left[\frac{\langle\delta(\boldsymbol{r}_1)\rangle}{m_0} + \frac{\langle\delta(\boldsymbol{r}_{12})\rangle}{m_2}\right] - \frac{14}{3}\left[\frac{Q(r_1)}{m_0} + \frac{Q(r_{12})}{m_2}\right]\right\}, \tag{29}$$

where $Q(r)$ is the Q term introduced by Araki[102] and Sucher.[103] Summarizing all the contributions of order $R_\infty\alpha^3$, one obtains

$$\begin{aligned} E^{(3)} &= E_{\rm se}^{(3)} + E_{\rm anom}^{(3)} + E_{\rm vp}^{(3)} + E_{\rm tr-ph}^{(3)} \\ &= \alpha^3\left\{\frac{4}{3}\left[-\ln\alpha^2 - \beta(v,L) + \frac{19}{30}\right]\left[\langle\delta(\boldsymbol{r}_1)\rangle + \langle\delta(\boldsymbol{r}_{12})\rangle\right] \right. \\ &\quad + \frac{2}{3}\left[-\ln\alpha - 4\beta(v,L) + \frac{31}{3}\right]\left[\frac{\langle\delta(\boldsymbol{r}_1)\rangle}{m_0} + \frac{\langle\delta(\boldsymbol{r}_{12})\rangle}{m_2}\right] \\ &\quad \left. - \frac{14}{3}\left[\frac{Q(r_1)}{m_0} + \frac{Q(r_{12})}{m_2}\right]\right\}. \end{aligned} \tag{30}$$

In the basis set of Eq. (9), the Q terms can be expressed as[104]

$$Q(r_1) = \lim_{\varepsilon\to 0}\left\langle\frac{\Theta(r_1-\varepsilon)}{4\pi r_1^3} + (\ln\varepsilon + \gamma_{\rm E})\delta(\boldsymbol{r}_1)\right\rangle, \tag{31}$$

$$Q(r_{12}) = \lim_{\varepsilon\to 0}\left\langle\frac{\Theta(r_{12}-\varepsilon)}{4\pi r_{12}^3} + (\ln\varepsilon + \gamma_{\rm E})\delta(\boldsymbol{r}_{12})\right\rangle, \tag{32}$$

where $\gamma_{\rm E}$ is Euler's constant, ε is the radius of a sphere about $r=0$ to be excluded from the integration for $Q(r)$. Numerical values of these terms can be found in Table 5 and Table 6 for H_2^+ and HD^+, respectively.

Table 5. Numerical values of $Q(r_1)$ for H_2^+, where $v = 0$–4 and $L = 0$–4.

$L\backslash v$	0	1	2	3	4
0	–0.13442622791325256(8)	–0.131286375375801(2)	–0.128392575302857(4)	–0.125731500111197(2)	–0.123291681209024(4)
1	–0.1342668168626330(4)	–0.131136925403617(2)	–0.12825265604664(3)	–0.12560074245121(4)	–0.123169774407(2)
2	–0.133950459810467(2)	–0.13084038002659(3)	–0.12797506716106(2)	–0.125341377055(1)	–0.122928016028(1)
3	–0.133481987355(3)	–0.13040135187(2)	–0.12756421444(3)	–0.12495761350(4)	–0.1225704297(3)
4	–0.132868404802(1)	–0.12982652672(1)	–0.1270264810(1)	–0.12445554797(5)	–0.122102840(2)

Table 6. Numerical values of $Q(r_1)$ and $Q(r_{12})$ for HD^+, where $v = 0$–4 and $L = 0$–4. For each (v,L), the first entry is for $Q(r_1)$ and the second is for $Q(r_{12})$.

$L\backslash v$	0	1	2	3	4
0	–0.1348622766081903(2)	–0.132113355129(1)	–0.129551987571271(1)	–0.1271692904455(1)	–0.124957495577393(3)
	–0.1345911955685105(1)	–0.131838977797(3)	–0.129272929986259(7)	–0.126883928318(2)	–0.124663886878278(6)
1	–0.134742001057392(5)	–0.13199961143967(2)	–0.1294445278685(4)	–0.1270678977803(2)	–0.124861982784(2)
	–0.13447097875759(1)	–0.131725268104580(5)	–0.1291654760689(3)	–0.126782508560(1)	–0.124568307802(8)
2	–0.13450284686085(8)	–0.1317734666211(3)	–0.1292308990657(3)	–0.126866353373(3)	–0.124672150627(1)
	–0.134231940231203(3)	–0.1314991894516(1)	–0.1289518569532(7)	–0.126580907975(1)	–0.124378340936(7)
3	–0.1341475653900(1)	–0.131437564457(6)	–0.12891364214(1)	–0.12656709998(4)	–0.124390349(3)
	–0.133876827784(1)	–0.13116338201(2)	–0.12863460989(3)	–0.1262815656(3)	–0.12409633(1)
4	–0.1336801802328(6)	–0.130995769843(4)	–0.128496470584(6)	–0.12617370653(3)	–0.1240200070(4)
	–0.133409659744(2)	–0.13072170536(5)	–0.12821744286(1)	–0.1258880438(2)	–0.123725701795(5)

The Bethe logarithm $\beta(v,L)$, the most difficult to calculate, is responsible for the nonrelativistic part of the self-energy of a charged particle in a quantum state interacting with transverse photons. The Bethe logarithm can either be represented by a sum over intermediate states[95,105] or by an integral over intermediate photon momentum k,[106] according respectively to

$$\begin{aligned}\beta(v,L) &\equiv \frac{\mathcal{N}(v,L)}{\mathcal{D}(v,L)} \\ &= \frac{\sum_i |\langle\psi_0|\boldsymbol{J}|\psi_i\rangle|^2 (E_i-E_0)\ln|E_i-E_0|}{\sum_i |\langle\psi_0|\boldsymbol{J}|\psi_i\rangle|^2 (E_i-E_0)}, \qquad (33) \\ &= \frac{1}{\mathcal{D}(v,L)} \lim_{K\to\infty} \left(-K\langle\psi_0|\boldsymbol{J}^2|\psi_0\rangle + \mathcal{D}(v,L)\ln K \right. \\ &\quad \left. + \int_0^K k\,\mathrm{d}k \langle\psi_0|\boldsymbol{J}(H_0-E_0+k)^{-1}\boldsymbol{J}|\psi_0\rangle \right), \qquad (34)\end{aligned}$$

where $|\psi_0\rangle$ is the energy eigenstate of interest with the corresponding energy eigenvalue E_0; $\boldsymbol{J}=\sum_a q_a \boldsymbol{P}_a/m_a$ is the electric current density operator of the system with q_a, $\boldsymbol{P}_a$, and m_a being respectively the charge, the momentum operator relative to a laboratory coordinate system, and the mass of particle a; the summation over i covers all virtual intermediate states connected to $|\psi_0\rangle$ by the operator $\boldsymbol{J}$; and $(H_0-E_0+k)^{-1}$ is the resolvent operator associated with the nonrelativistic Hamiltonian H_0. Korobov[107] applied the approach of Schwartz[106] to evaluate $\beta(v,L)$ for the hydrogen molecular ions according to Eq. (34) and obtained about 5–6 significant digits for HD^+[108] and H_2^+.[109] In 2012, a further development on the Schwartz approach was made by Korobov[110,111] to deal with a general three-body system, such as helium, H_2^+, and HD^+, in which the dipole matrix elements are expressed in the velocity gauge. After that, this method was applied to H_2^+ and HD^+ by Korobov and Zhong[81] for the rovibrational states of $v=0$–4 and $L=0$–4. Besides the Schwartz approach, Drake and Goldman[112] developed a different method for the calculation of the Bethe logarithm for the case of atomic systems. Their method only requires a single matrix diagonalization of the Hamiltonian in a basis set containing a wide range of distance scales. The Drake–Goldman method was successfully applied to H_2^+ by Zhong *et al.*[113] for $v=0$–1 and $L=0$. The precision achieved for these two states is a few parts in 10^9, which demonstrates the feasibility of the Drake–Goldman method for simple molecular systems. The details of the calculations of $\beta(v,L)$ can be found in Ref. [110] for the Schwartz method and in Ref. [113] for the Drake–Goldman method. The latest numerical values of $\beta(v,L)$ can be found in Refs. [81] and [113] that are quoted in Table 7 and Table 8.

Table 7. Bethe logarithms for low-lying rovibrational states of H_2^+, see Table 4 of Ref. [81].

$L\backslash v$	0	1	2	3	4
0	3.012230335(1)	3.012547548(3)	3.01267873(2)	3.01262269(4)	3.01237775(6)
	3.012230329(7) [a]	3.012547533(3) [a]			
1	3.01220132(1)	3.01251393(2)	3.01264054(3)	3.01258051(4)	3.0123316(1)
2	3.01214395(1)	3.01244742(2)	3.01256542(3)	3.01249674(4)	3.0122395(1)
3	3.01205949(2)	3.01234936(3)	3.01245429(4)	3.01237302(5)	3.0121036(1)
4	3.01194983(3)	3.01222182(3)	3.01230955(5)	3.01221169(6)	3.0119263(2)

[a] Ref. [113]

Table 8. Bethe logarithms for low-lying rovibrational states of HD^+, see Table 5 of Ref. [81].

$L\backslash v$	0	1	2	3	4
0	3.01233626(2)	3.01263268(3)	3.01278948(4)	3.01280622(6)	3.0126822(1)
1	3.01231470(2)	3.01260814(3)	3.01276198(5)	3.0127760(1)	3.0126490(1)
2	3.01227206(2)	3.01255942(3)	3.01270766(5)	3.0127160(1)	3.0125836(2)
3	3.01220877(3)	3.01248727(4)	3.01262691(6)	3.0126269(1)	3.0124865(2)
4	3.01212616(4)	3.01239292(4)	3.0125211(1)	3.0125102(1)	3.0123593(2)

2.4. $R_\infty\alpha^4$ order corrections

The corrections of order $R_\infty\alpha^4$ are also needed to be taken into consideration.[31,114,115] However, the recoil corrections of order $R_\infty\alpha^4(m_e/m_{nuc})$ and higher are small and can be neglected at the precision of ~ 0.01–0.1 ppb. The self-energy and the vacuum polarization corrections at this order are respectively

$$E_{se}^{(4)} = \alpha^4\left\{4\pi\left(\frac{139}{128}-\frac{1}{2}\ln 2\right)[\langle\delta(\boldsymbol{r}_1)\rangle+\langle\delta(\boldsymbol{r}_{12})\rangle]\right\}, \qquad (35)$$

and

$$E_{vp}^{(4)} = \alpha^4\left\{\left(\frac{5\pi}{48}-\frac{82}{81\pi}\right)[\langle\delta(\boldsymbol{r}_1)\rangle+\langle\delta(\boldsymbol{r}_{12})\rangle]\right\}. \qquad (36)$$

Note that in Ref. [31], the above term $-\frac{82}{81\pi}$ of the vacuum polarization is incorporated into Eq. (38) below. The contribution from the anomalous magnetic moment of order $R_\infty\alpha^4$ is

$$E_{anom}^{(4)} = \alpha^4\left\{\left[\frac{197}{144}+\frac{\pi^2}{12}-\frac{\pi^2}{2}\ln 2+\frac{3}{4}\zeta(3)\right]\right.$$

$$\times[\langle\delta(r_1)\rangle+\langle\delta(r_{12})\rangle]\Big\}. \tag{37}$$

Finaly the contribution due to the second-order slope of the Dirac form factor is

$$E^{(4)}_{\rm 2loop} = \frac{\alpha^4}{\pi}\left\{\left[-\frac{4819}{1296}-\frac{49\pi^2}{108}+2\pi^2\ln 2-3\zeta(3)\right] \times[\langle\delta(r_1)\rangle+\langle\delta(r_{12})\rangle]\right\}. \tag{38}$$

Summing up all the contributions, the total radiative correction of order $R_\infty\alpha^4$ in the external field approximation can be expressed as

$$\begin{aligned} E^{(4)}_{\rm rad} &= E^{(4)}_{\rm se}+E^{(4)}_{\rm vp}+E^{(4)}_{\rm anom}+E^{(4)}_{\rm 2loop} \\ &= \alpha^4\left\{\frac{1}{\pi}\left[-\frac{2179}{648}+\frac{3523}{864}\pi^2-\frac{1}{2}\pi^2\ln 2-\frac{9}{4}\zeta(3)\right] \times[\langle\delta(r_1)\rangle+\langle\delta(r_{12})\rangle]\right\}. \end{aligned} \tag{39}$$

Currently, the order $R_\infty\alpha^4$ relativistic corrections are calculated in the two-center approximation.[31,116] In this approximation, the Hamiltonian of the nonrelativistic Schrödinger equation is expressed as

$$H_0=-\frac{\nabla^2}{2}+V,\quad V=-\frac{1}{r_1}-\frac{1}{r_2}+\frac{1}{R}, \tag{40}$$

where R is the distance between the two nuclei, and r_1 and r_2 are the distances from the electron to nuclei 1 and 2, respectively. The total relativistic correction to the energy of a bound electron at order $R_\infty\alpha^4$ is calculated according to

$$E^{(4)}_{\rm rel}=\alpha^4\langle H_{\rm B}Q(E_0-H_0)^{-1}QH_{\rm B}\rangle+\alpha^4\langle H^{(4)}_{\rm eff}\rangle, \tag{41}$$

where $Q=1-|\psi_0\rangle\langle\psi_0|$ is the projection operator and $H_{\rm B}$ is the Breit–Pauli Hamiltonian defined by

$$H_{\rm B} = -\frac{\nabla^4}{8}+\frac{4\pi}{8}[\delta(r_1)+\delta(r_2)] -{\rm i}\left(\frac{r_1}{r_1^3}\times\nabla+\frac{r_2}{r_2^3}\times\nabla\right)\cdot s. \tag{42}$$

The effective Hamiltonian $H^{(4)}_{\rm eff}$ represents the interaction of the bound electron with the external field generated by the two nuclei and has the form of

$$H^{(4)}_{\rm eff} = -\frac{\nabla^6}{16}+\frac{(\mathcal{E}_1+\mathcal{E}_2)^2}{8}+\frac{3\pi}{16}[\nabla^2\rho+\rho\nabla^2] +\frac{5}{128}(\nabla^4V+V\nabla^4)-\frac{5}{64}(\nabla^2V\nabla^2), \tag{43}$$

where $\mathcal{E}_i=-r_i/r_i^3$ and $\rho=\delta(r_1)+\delta(r_2)$. It should be mentioned that both terms in Eq. (41) are divergent and the details for a complete removal of the divergence between these two terms can be found in Ref. [116]. The final finite result is

$$E^{(4)}_{\rm rel} = \alpha^4\langle H'_{\rm B}Q(E_0-H_0)^{-1}QH'_{\rm B}\rangle+\alpha^4\frac{3E_0\langle V^2\rangle}{4} -\alpha^4\frac{5E_0^2\langle V\rangle}{4}-\alpha^4\frac{3\pi E_0\langle\rho\rangle}{4}-\alpha^4\frac{\langle\nabla V^2\nabla\rangle}{8} +\alpha^4\frac{\langle V\rangle\langle H_{\rm B}\rangle}{2}+\alpha^4\frac{E_0^3}{2}, \tag{44}$$

which can be evaluated numerically. The numerical values of $E^{(4)}_{\rm rel}$ are listed in Table 9 and Table 10 for H_2^+ and HD^+, respectively.[31] Finally the total correction of this order is

$$E^{(4)}=E^{(4)}_{\rm rad}+E^{(4)}_{\rm rel}. \tag{45}$$

Table 9. Relativistic corrections of order $R_\infty\alpha^4$ for H_2^+. Units are α^4 a.u.

$L\backslash v$	0	1	2	3	4
0	–0.042097	–0.042908	–0.043786	–0.044732	–0.045729
1	–0.042100	–0.042912	–0.043792	–0.044740	–0.045738
2	–0.042107	–0.042922	–0.043805	–0.044757	–0.045756
3	–0.042117	–0.042938	–0.043825	–0.044782	–0.045783
4	–0.042133	–0.042959	–0.043854	–0.044818	–0.045820

Table 10. Relativistic corrections of order $R_\infty\alpha^4$ for HD^+. Units are α^4 a.u.

$L\backslash v$	0	1	2	3	4
0	–0.042043	–0.042738	–0.043483	–0.044278	–0.045126
1	–0.042045	–0.042741	–0.043487	–0.044284	–0.045132
2	–0.042050	–0.042748	–0.043496	–0.044295	–0.045146
3	–0.042058	–0.042759	–0.043510	–0.044312	–0.045167
4	–0.042069	–0.042773	–0.043529	–0.044336	–0.045195

2.5. $R_\infty\alpha^5$ order corrections

The next order of corrections that we should consider is $R_\infty\alpha^5$, which contain the contributions of the self-energy, the vacuum polarization, the Wichman–Kroll term, the complete two-loop diagrams, and the three-loop diagrams. The $R_\infty\alpha^5$ order corrections for hydrogenlike ions can be found in Refs. [114], [115], and [117]. In early times, these corrections were calculated in the hydrogen approximation where the parameters of hydrogen were adopted.[30,31] In 2014, the $R_\infty\alpha^5$ order corrections were extended by Korobov *et al.*[83,84] to a system of two Coulomb centers. Thus the two-center approximation used for the $R_\infty\alpha^4$ order relativistic corrections will also be used in the following equations.

The main part of this shift is the self-energy contribution. The general results obtained in Refs. [118]–[120] for a bound electron in an external field were taken as the starting point in the work of Korobov *et al.* Since in Refs. [118]–[120] the form of field is generic, it is possible to extend their approach to the two-center problem. The details of the derivation can be found in Ref. [84]. The final result is

$$E^{(5)}_{\rm se}=\alpha^5\langle\rho\rangle[A_{60}+A_{61}\ln(\alpha^{-2})+A_{62}\ln^2(\alpha^{-2})], \tag{46}$$

where $A_{62}=-1$, and the expressions of A_{60} and A_{61} are

$$A_{60}(R) = \left[\left(\frac{5}{9}-\frac{2}{3}\ln 2\right)\langle 4\pi\rho Q(E_0-H_0)^{-1}QH_{\rm B}\rangle_{\rm fin} +\left(\frac{779}{14400}-\frac{11}{120}\ln 2\right)\langle\nabla^4V\rangle_{\rm fin}\right.$$

$$+\left(\frac{589}{720}-\frac{2}{3}\ln 2\right)\langle(\nabla V)^2\rangle_{\rm fin}-\frac{3}{80}\langle 4\pi\rho\nabla^2\rangle_{\rm fin}$$
$$-0.81971202(1)\pi\langle\rho\rangle+\mathcal{L}(R)\Big]\Big/\langle\rho\rangle, \quad (47)$$

$$A_{61}(R) = \Big[\frac{2}{3}\langle 4\pi\rho Q(E_0-H_0)^{-1}QH_{\rm B}\rangle_{\rm fin}+\frac{11}{120}\langle\nabla^4 V\rangle_{\rm fin}$$
$$+\frac{2}{3}\langle(\nabla V)^2\rangle_{\rm fin}+\left(\frac{16}{3}\ln 2-\frac{1}{4}\right)\langle\rho\rangle\Big]\Big/\langle\rho\rangle. \quad (48)$$

In the above, $\langle\ \rangle_{\rm fin}$ means that the matrix elements are redefined in finite forms, and the other notations can be found in Section 2.4. The most difficult part to calculate is the relativistic Bethe logarithm $\mathcal{L}(R)$, which has been evaluated by Korobov and coworkers[82] for the two-center problem. For the vacuum polarization in a strong external field, the leading-order correction is the Uehling term,

$$E_{\rm vp}^{(5)}=\alpha^5[V_{60}+V_{61}\ln(\alpha^{-2})]\langle\rho\rangle, \quad (49)$$

which contributes at the level of 1 kHz and can thus be estimated in the hydrogen approximation. The coefficients for an S state of the atomic hydrogen are

$$V_{60}(nS) = \frac{4}{15}\Big[-\frac{431}{105}+\psi(n+1)-\psi(1)$$
$$-\frac{2(n-1)}{n^2}+\frac{1}{28n^2}-\ln\frac{n}{2}\Big],$$
$$V_{61}(nS) = -\frac{2}{15}, \quad (50)$$

where $V_{60}(n{\rm S})$ is taken from Refs. [121]–[124] and $V_{61}(n{\rm S})$ from Ref. [125]. The Wichman–Kroll term[126] can be expressed in the form

$$E_{\rm WK}^{(5)}=\alpha^5 W_{60}\langle\rho\rangle,\quad W_{60}(n{\rm S})=\frac{19}{45}-\frac{\pi^2}{27}. \quad (51)$$

The next contribution is the complete two-loop Feynman diagrams[127–129]

$$E_{\rm 2loop}^{(5)}=\frac{\alpha^5}{\pi}B_{50}\langle\rho\rangle, \quad (52)$$

where $B_{50}=-21.55447(12)$. This expression is valid for a bound electron in an arbitrary configuration of a few pointlike Coulomb sources. The contribution from the three-loop Feynman diagrams at this order is[130–133]

$$E_{\rm 3loop}^{(5)}=\frac{\alpha^5}{\pi^2}0.42\langle\rho\rangle, \quad (53)$$

which may be negligible. The total contribution of order $R_\infty\alpha^5$ is therefore

$$E^{(5)}=E_{\rm se}^{(5)}+E_{\rm vp}^{(5)}+E_{\rm WK}^{(5)}+E_{\rm 2loop}^{(5)}+E_{\rm 3loop}^{(5)}. \quad (54)$$

In addition to these corrections discussed above, the dominant part of $R_\infty\alpha^6$ is also considered, which represents the second-order perturbation with two one-loop self-energy operators

$$E^{(6)}=\frac{\alpha^6}{\pi}\left(-\frac{8}{27}\right)\ln^3(\alpha^{-2})\langle\rho\rangle. \quad (55)$$

2.6. Finite nuclear size effects

The electron in the hydrogen molecular ion is settled in the $1\sigma_g$ state with its principal quantum number $n=1$ and the angular momentum quantum number $l=0$. In the hydrogen approximation, it can be simplified as a 1s state. Thus, we can calculate the corrections of the finite nuclei size using the formula for the s-state hydrogen or deuterium. According to Refs. [114] and [115], the leading-order correction of the finite nuclear size is given by

$$E_{\rm nuc-1}=\frac{2\pi}{3}\sum_{i=0,2}R_i^2\langle\delta(\boldsymbol{r}_i)\rangle, \quad (56)$$

where R_0 and R_2 are the root-mean-square radii of the two nuclear charge distributions. It is $R_{\rm p}=0.8775(51)$ fm for the proton and $R_{\rm d}=2.1424(21)$ fm for the deuteron.[6] The next-order correction is given by (see Ref. [6] and references therein)

$$E_{\rm nuc-2}=-\frac{2\pi}{3}\sum_{i=0,2}C_\eta^{(i)}m_iR_i^3\langle\delta(\boldsymbol{r}_i)\rangle, \quad (57)$$

where $C_\eta^{(i)}$ are constants that depend on the charge distributions in the nuclei with $C_\eta^{(p)}=1.7(1)$ for the proton and $C_\eta^{(d)}=2.0(1)$ for the deuteron. The leading-order correction $E_{\rm nuc-1}$ has been evaluated in earlier works,[30,79,80] while $E_{\rm nuc-2}$ has not been considered before. We found that $E_{\rm nuc-2}$ can have a noticeable contribution to a transition frequency at the current required precision. The remaining corrections of the finite nuclear size are at the level of Hz or smaller and can thus be neglected. Finally, the total correction due to the finite nuclear size is

$$E_{\rm nuc}=E_{\rm nuc-1}+E_{\rm nuc-2}. \quad (58)$$

2.7. Total transition frequency

The total transition frequency is obtained by summing up all the contributions

$$\Delta E_{\rm total} = E_{\rm f}-E_{\rm i}=\Delta E_{\rm nr}+\Delta E_{\rm nuc}+\Delta E^{(2)}$$
$$+\Delta E^{(3)}+\Delta E^{(4)}+\Delta E^{(5)}+\Delta E^{(6)}, \quad (59)$$

where $E_{\rm i}$ and $E_{\rm f}$ are the energy levels of the initial and final states, respectively. Table 11 lists individual contributions up to $R_\infty\alpha^6$ to the fundamental transition $(v,L):(0,0)\to(1,0)$ in H_2^+ and HD^+. The nonrelativistic energies and the leading-order relativistic corrections were calculated by using the fundamental physical constants of the 2010 CODATA set.[6] The uncertainty of $\Delta E_{\rm nr}$ comes from the uncertainty of the Hartree energy $E_{\rm h}$.[6] It should be pointed out that the uncertainty in $\Delta E^{(2)}$ is entirely due to the fundamental physical constants used. Also listed in Table 11 is the earlier value of $\Delta E^{(2)}$ for H_2^+[79] calculated using the 2006 CODATA recommended

values,[134] which has a slight discrepancy of about 10 Hz. The computational uncertainty in $\Delta E^{(2)}$ can be ignored due to the high precision numerical values of the energy levels in Table 1. The remaining uncertainty in $\Delta E^{(2)}$ is from the uncertainty of the Rydberg constant R_∞ due to the unit conversion, which is less than the total uncertainty in the transitional frequency and will not affect the m_p/m_e determination at the present targeted precision. The current uncertainty of $\Delta E^{(3)}$ is mainly due to the numerical uncertainties of the Bethe logarithm. For HD^+, the uncertainty of $\Delta E^{(3)}$ was reduced from 40 Hz[81] to 8 Hz because the high precision values of the Q term were adopted. The uncertainty in $\Delta E^{(4)}$ is due to $E^{(4)}_{\rm rel}$, which was estimated to be $10^{-5}\alpha^4$ a.u. The uncertainty in the $\Delta E^{(5)}$ term was reduced from 20 kHz to 2 kHz because of the improved calculation of the one-loop self-energy.[83,84] Finally the uncertainty in $\Delta E^{(6)}$ was estimated by the two one-loop self-energy corrections and its magnitude is smaller than the uncertainty of the $\Delta E^{(5)}$ term. The finite nuclear size effect has a significant contribution to the transition frequency. In early works, only the leading-order finite-nuclear size correction was calculated. We estimated that the next order correction has a contribution beyond the uncertainty of the $\Delta E^{(5)}$ correction and it should be taken into account. As a result, the present value of $\Delta E_{\rm nuc}$ is different from the previous one. This in turn leads to a difference in the total frequency by about 20 to 30 kHz from the latest calculations of Korobov and coworkers.[83,84] It is, however, that the $R_\infty\alpha^5$ order correction remains the source of uncertainty in the total transition frequency.

Table 11. Summary of contributions to the transition frequency $(v,L):(0,0)\rightarrow(1,0)$ of H_2^+ and HD^+. Units are MHz.

	H_2^+	HD^+
$\Delta E_{\rm nr}$	65687511.071 42(17)	57349439.97334(15)
$\Delta E^{(2)}$	1 091.081365(7)	958.276694(8)[80]
	1 091.081355(2)[79]	
	1 091.081(03)[a]	958.277(01)[a]
$\Delta E^{(3)}$	–276.545038(12)[b]	–242.126263(8)
	–276.545049(4)[81]	–242.12626(4)[81]
	–276.544(02)[30]	–242.125(02)[30]
$\Delta E^{(4)}$	–1.99730(26)[c]	–1.74837(26)[c]
$\Delta E^{(5)}$	0.138(2)[83,84]	0.120(2)[83,84]
	0.120(23)[31]	0.105(19)[31]
$\Delta E^{(6)}$	0.001(1)[83,84]	0.001(1)[83,84]
$\Delta E_{\rm nuc}$	–0.03899(50)	–0.0924(16)
	–0.0410(6)[79]	–0.1252(17)[80]
	–0.0410(3)[a]	–0.125(2)[a]
$\Delta E_{\rm total}$	65 688323.710 5(28)	57350154.404 0(28)
[83,84]	65688323.708(2)	57350154.371(2)
[80]		57350154.355(22)
[31]	65688323.688(25)	57350154.355(21)
[30]	65688323.745(80)	57350154.412(70)

[a] Obtained using the data of Table V in Ref. [30].
[b] Obtained using the values of the Bethe logarithm from Ref. [80].
[c] Obtained using the values of the $R_\infty\alpha^4$ corrections from Ref. [31].

Table 12 lists some important transition frequencies in HD^+, together with the available experimental measurements. For the transition $(v,L):(0,0)\rightarrow(1,1)$, there is a discrepancy of about 150 kHz between theory and experiment. At first glance, this seems to be introduced by the higher-order correction of the finite nuclear size effect that is ignored in previous works. However, this correction to $(v,L):(0,0)\rightarrow(1,1)$ is estimated to be only +34 kHz, indicating that the resulting discrepancy is now increased to 180 kHz. The reason for this discrepancy is unknown.

Table 12. Theoretical and experimental transition frequencies in HD^+. The last two measurements are currently underway.[27,135] Units are MHz.

$(v,L)\rightarrow(v',L')$	Experiment	Theory
(0,2)→(4,3)	214978560.6(5)[23]	214978560.948(8)[83,84]
(0,0)→(1,1)	58605052.00(6)[26]	58605052.156(2)[83,84]
(0,0)→(0,1)	[135]	1314925.7523(1)[84]
(0,2)→(8,3)	[27]	383407177.150(15)[84]

3. Experiment

3.1. Sympathetic cooling of hydrogen molecular ions

The motion-induced Doppler broadening is the main factor affecting the precision and resolution of rovibrational spectroscopy in the hydrogen molecular ions. Reducing the translational energy of the ions and confining them in the Lamb–Dicke region can minimize the first-order Doppler shift and broadening to the greatest extent.[25]

The complexity of the molecular energy level structure usually prevents the implementation of closed optical cycles so that laser cooling is generally not applicable to molecules or molecular ions. Over the past 15 years, sympathetic cooling[136,137] has emerged as a versatile method for cooling a broad range of molecular ions to millikelvin secular temperatures with laser-cooled atomic ions.[138–140] Since the molecular ions can exchange kinetic energy with the laser-cooled atomic species by Coulomb interactions, it is possible to reduce the molecular ions' kinetic energy. Thus, the atomic-ion species act as a coolant for the molecular ions resulting in the formation of bi-component (or molecular) Coulomb crystals.

The hydrogen molecular ions can be sympathetically cooled either using laser-cooled beryllium ions Be^+ or magnesium ions Mg^+. Due to the lower mass ratio between Be^+ and HD^+, using Be^+ as a coolant can provide higher cooling efficiency and lower secular temperature than using Mg^+. However, making a radiation source for laser cooled Be^+ is technologically demanding; on the other hand, using laser cooled Mg^+ as a coolant for sympathetically cooling HD^+ has advantages in terms of experimental complexity and cost.

Early theoretical work[141] gives the critical mass ratio for using heavy ions to sympathetically cool light ions, but this theoretical threshold has been overcome experimentally.[142] The more reliable method to determine the feasibility of performing high-efficiency sympathetic cooling between different ions is the use of molecular dynamics (MD) to simulate such a cooling process. An MD simulation can also provide

the characteristic information of molecular Coulomb crystal, e.g., the number of the laser-cooled and sympathetically cooled ions and their translational energies. We simulated 150 laser-cooled Mg^+ ions to sympathetically cool ten HD^+ ions and obtained an image of bi-component Coulomb crystal (see Fig. 4). The result shows that HD^+ can be sympathetically cooled into the Mg^+ Coulomb crystal and form a chain of almost stationary ($T \leq 10$ mK) molecular ions. At this temperature, the resolution of rovibrational spectroscopy of HD^+ can be obtained in about 10 MHz range. As we know, the spectral linewidth resulting from the Doppler broadening is proportional to $\sqrt{T}$; thus, the spectral precision will be similar using either laser-cooled Mg^+ or Be^+ species as a coolant.

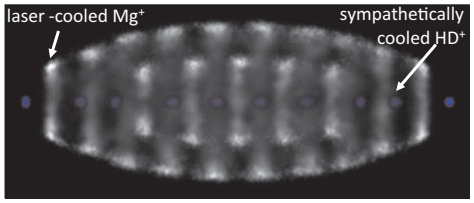


Fig. 4. Molecular dynamics simulation of a fluorescence image of an Mg^+/HD^+ bi-component Coulomb crystal. The spatial distribution of the non-fluorescing molecular HD^+ ions has been made visible in blue in the simulated image.

3.2. State preparation of HD^+ rovibrational levels

Translationally cold molecular ions are conventionally produced from "warm" samples by sympathetic cooling. Because low-energy collisions between ions are dominated by the Coulomb interaction which does not couple to the internal degrees of freedom, sympathetically cooled ions exhibit a broad distribution of the rotational-state population.[143,144] In such translationally cold but internally warm samples, the population can be accumulated in the rotational ground state using optical pumping scheme as demonstrated by Drewsen *et al.*[139] and Schneider *et al.*[87] Although optical pumping can increase the population of the rovibrational ground state by an order of magnitude higher than the corresponding thermal population at room temperature, the state preparation is not complete. A novel method has been developed to prepare internally state-selected molecular ions in a linear Paul ion trap.[143,144] The technique relies on the generation of molecular ions in a well-defined rovibrational quantum state using photoionization followed by sympathetic cooling of the translational motion with laser-cooled atomic ions.

Such a technique can be applied to prepare a single rovibrational quantum state in HD^+ by resonance-enhanced threshold photoionization (RETPI) method.[145] The experimental process includes the following three steps, as depicted in Fig. 5. First, neutral HD molecules are accumulated at low rovibrational states in a molecular beam due to the adiabatic expansion; second, an excitation laser of $\lambda_1 \approx 327$ nm is applied to populate HD to an exited electronic state. Finally, by setting a photoionization photon energy of $\lambda_2 \approx 314$ nm slightly above the desired ionic state accessible by the selection rules, HD^+ ions can be generated in a single rovibrational level.

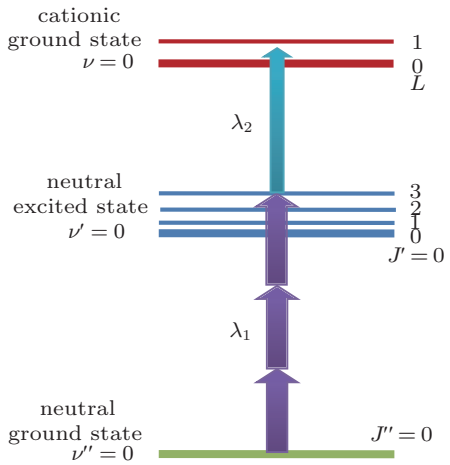


Fig. 5. State selective [3+1′] resonance-enhanced threshold-photoionization scheme used to generate HD^+ ions in the rovibrational ground state.

Since the RETPI method can produce molecular ions selectively due to the propensity rule of the excitation and ionization, it avoids generating undesired high abundant molecular species, such as H_2^+, MgH^+, and MgD^+. Furthermore, the relative spectral intensities need to be precisely measured for the determination of spectral line positions. The RETPI method ensures that all HD^+ ions are prepared in a single rovibrational quantum state and a transition from such a single state would offer the highest possible detecting sensitivity and the most accurate relative intensity. Previous measurements on HD^+ rovibrational transitions have improved the accuracy from 2 ppb to 1.1 ppb by using rotational cooling to increase the ground-state population.[84] We expect that the accuracy of the line position could further be improved to 0.4 ppb if a pure ionic species and a single rovibrational state could be obtained by using the RETPI method.

3.3. Measurement of HD^+ rovibrational spectroscopy

High-resolution infrared spectroscopy on sympathetically cooled HD^+ ions can be performed by using resonance-enhanced multiphoton dissociation (REMPD) spectroscopy.[23,146] The rovibrational transition $(v, L) : (0,0) \rightarrow (6,1)$ can be measured by using a single photon excitation at 991 nm. The absorption of an additional 355 nm photon from the vibrationally excited state results in photofragmentation of the ions. By comparing with an MD simulation, the rate of fragmentation can be derived from the time-resolved image change of the bi-component Coulomb crystal.

The probability of vibrational overtone transitions is much lower than the fundamental transitions. For example, the probabilities of transitions from $v : 0 \rightarrow 4$ and $v : 0 \rightarrow 8$ are 4 and 7 orders of magnitude lower than the fundamental transition of $v : 0 \rightarrow 1$ respectively. However, the sympathetically cooled molecular ions are spatially stationary ($T \sim$ mK,

trapping time ∼ hours), which can provide a minute-long interaction time between photons and ions. This unprecedentedly long interaction time ensures successful excitation of the vibrational overtone transitions.

In 2007, Schiller's group observed the overtone transitions of $v:0\rightarrow 4$ in HD^+ at the rate of 22 s^{-1} using a laser with 170 μW in power and 200 μm of beam waist.[23] The Einstein coefficient B of the $v:0\rightarrow 6$ transition is proximately $1/400$ of the transition $v:0\rightarrow 4$. We estimate the rate of transition by employing a laser of 100 kHz linewidth, 100 mW in power, and 200 μm beam waist to be achieved at 64 s^{-1}, which is faster than the other observed overtone transitions of $v:0\rightarrow 8$.[27] The hyperfine transition linewidth in sympathetically cooled HD^+ ions is around 10 MHz, which is dominated by the Doppler broadening of the residual thermal energy. The radiation intensity of the above proposed laser system would not bring an additional broadening of the measured transition linewidth. The uncertainty of the induced AC Stark shift is on the order of 10^{-12}, which will evidently not affect the targeted accuracy.

4. Summary

The past few years have witnessed impressive progress in the field of sympathetic cooling of molecular ions. New experimental methods have been developed, which allow for an effective control of molecular internal quantum sates. Such developments have opened up a variety of opportunities for spectroscopic measurements of molecular ions with high precision. In our project/proposal, the hydrogen molecular ions HD^+ can be generated to the rovibrational ground state by RETPI, and can be sympathetically cooled to millikelvin by laser-cooled atomic ions. With this accurate control of internal and external degrees of freedom, the overtone transition frequency from the rovibrational ground state to the 6th rovibrational excited state can be determined by the REMPD method. The relative accuracy of the measured transition frequency around 991 nm is expected to reach 0.4 ppb.

On the theoretical side, the contributions up to $R_\infty\alpha^5$ have been taken into account in the calculations of the transition frequencies of H_2^+ and HD^+. Thanks to the significant work of Korobov and coworkers,[82–84] the uncertainties of the theoretical results have been reduced from 80 kHz to 2 kHz for some important transitions. The relative uncertainties of theoretical values have been improved by about one order of magnitude, reaching the level of 0.03 ppb for H_2^+ and HD^+. The current theoretical transition frequencies can be used to derive an improved value of the proton-to-electron mass ratio,[6] once the experimental measurements for these transitions become available. Further refinement in theory may be made by performing improved calculation of the $R_\infty\alpha^4(m_e/m_{nuc})$ order recoil correction and the $R_\infty\alpha^5$ order correction, as well as by including higher-order finite nuclear size effects. Finally it is highly desirable to perform an independent evaluation of all high-order relativistic and radiative corrections.

Acknowledgments

We would like to thank Shu-Min Zhao, Li-Yan Tang, Pei-Pei Zhang, and Quan-Long Tian for their participation and contributions. We also thank Kelin Gao and Hua Guan for valuable discussion, and V. I. Korobov of JINR for his expertise and encouragement.

References

[1] Greiner W, Schramm S and Stein E 2004 *Quantum Chromodynamics* (2nd edn.) (Berline: Springer) pp. 178–182
[2] Schiller S and Korobov V 2005 *Phys. Rev. A* **71** 032505
[3] Karr J Ph, Bielsa F, Valenzuela T, Douillet A, Hilico L and Korobov V I 2007 *Can. J. Phys.* **85** 497
[4] Salumbides E J, Koelemeij J C J, Komasa J, Pachucki K, Eikema K S E and Ubachs W 2013 *Phys. Rev. D* **87** 112008
[5] Salumbides E J, Ubachs W and Korobov V I 2014 *Journal of Molecular Spectroscopy* **300** 65
[6] Mohr P J, Taylor B N and Newell D B 2012 *Rev. Mod. Phys.* **84** 1527
[7] Verdú J, Djekić S, Stahl S, Valenzuela T, Vogel M, Werth G, Beier T, Kluge H J and Quint W 2004 *Phys. Rev. Lett.* **92** 093002
[8] Sturm S, Köhler F, Zatorski J, Wagner A, Harman Z, Werth G, Quint W, Keitel C H and Blaum K 2014 *Nature* **506** 467
[9] Cärtner G and Klempt E 1978 *Z. Physik A* **287** 1
[10] Gräff G, Kalinowsky H and Traut J 1980 *Z. Physik A* **297** 35
[11] Van Dyck R S, Jr. and Schwinberg P B 1981 *Phys. Rev. Lett.* **47** 395
[12] Van Dyck R S, Jr., Moore F L, Farnham D L and Schwinberg P B 1985 *Int. J. Mass Spectrosc. Ion Proc.* **66** 327
[13] Farnham D L, Van Dyck R S, Jr. and and Schwinberg P B 1995 *Phys. Rev. Lett.* **75** 3598
[14] Wineland D J, Bollinger J J and Itano W M 1983 *Phys. Rev. Lett.* **50** 628
[15] Erratum 1983 *Phys. Rev. Lett.* **50** 1333
[16] Gabrielse G, Fei X, Orozco L A, Tjoelker R L, Haas J, Kalinowsky H, Trainor T A and Kells W 1990 *Phys. Rev. Lett.* **65** 1317
[17] Karshenboim S G 2005 *Phys. Rep.* **422** 1
[18] Karshenboim S G 2008 *Lect. Notes. Phys.* **745** 1
[19] Hayano R S, Hori M, Horváth D and Widmann E 2007 *Pep. Prog. Phys.* **70** 1995
[20] Hori M and Walz J 2013 *Prog. Part. Nucl. Phys.* **72** 206
[21] Hori M, Dax A, Eades J, Gomikawa K, Hayano R S, Ono N, Pirkl W, Widmann E, Torii H A, Juhász B, Barna D and Horváth D 2006 *Phys. Rev. Lett.* **96** 243401
[22] Hori M, Sótér A, Barna D, Dax A, Hayano R, Friedreich S, Juhász B, Pask T, Widmann E, Horváth D, Venturelli L and Zurlo N 2011 *Nature* **475** 484
[23] Koelemeij J C J, Roth B, Wicht A, Ernsting I and Schiller S 2007 *Phys. Rev. Lett.* **98** 173002
[24] Hori M and Walz J 2013 *Prog. Part. Nuc. Phys.* **72** 206
[25] Roth B, Koelemeij J, Schiller S, Hilico L, Karr J Ph, Korobov V I and Bakalov D 2008 *Lect. Notes Phys.* **745** 205
[26] Bressel U, Borodin A, Shen J, Hansen M, Ernsting I and Schiller S 2012 *Phys. Rev. Lett.* **108** 183003
[27] Koelemeij J C J, Noom D W E, de Jong D, Haddad M A and Ubachs W 2012 *Appl. Phys. B* **107** 1075
[28] Korobov V I 2003 *Phys. Rev. A* **67** 062501
[29] Erratum 2003 *Phys. Rev. A* **68** 019902
[30] Korobov V I 2006 *Phys. Rev. A* **74** 052506
[31] Korobov V I 2008 *Phys. Rev. A* **77** 022509
[32] Korobov V I 2008 *Phys. Rev. A* **77** 042506
[33] Blythe P, Roth B, Fröhlich U, Wenz H and Schiller S 2005 *Phys. Rev. Lett.* **95** 183002
[34] Bekbaev A K, Korobov V I and Dineykhan M 2011 *Phys. Rev. A* **83** 044501
[35] Tian Q L, Tang L Y, Zhong Z X, Yan Z C and Shi T Y 2012 *J. Chem. Phys.* **137** 024311
[36] Caswell W E and Lepage G P 1986 *Phys. Lett. B* **167** 437

[37] Nio M and Kinoshita T 1997 *Phys. Rev. D* **55** 7267
[38] Bates D R, Ledsham K and Stewart A L 1953 *Phil. Trans. R. Soc. A* **246** 215
[39] Carrington A, MacNab I R and Montgomerie C A 1989 *J. Phys. B* **22** 3551
[40] Leach C A and Moss R E 1995 *Ann. Rev. Phys. Chem.* **46** 55
[41] Bishop D M and Solunac S A 1985 *Phys. Rev. Lett.* **55** 1986
[42] Erratum 1985 *Phys. Rev. Lett.* **55** 2627
[43] Moss R E and Sadler I A 1989 *Mol. Phys.* **68** 1015
[44] Rebane T K and Filinsky A V 1997 *Phys. At. Nucl.* **60** 1816
[45] de Saavedra F A, Buendía E, Gálvez F J and Sarsa A 1998 *Eur. Phys. J. D* **2** 181
[46] Grémaud B, Delande D and Billy N 1998 *J. Phys. B* **31** 383
[47] Bhatia A K 1998 *Phys. Rev. A* **58** 2787
[48] Moss R E 1999 *J. Phys. B* **32** L89
[49] Taylor J M, Yan Z C, Dalgarno A and Babb J F 1999 *Mol. Phys.* **97** 25
[50] Hilico L, Billy N, Grémaud B and Delande D 2000 *Eur. Phys. J. D* **12** 449
[51] Korobov V I 2000 *Phys. Rev. A* **61** 064503
[52] Bailey D H and Frolov A M 2002 *J. Phys. B* **35** 4287
[53] Yan Z C, Zhang J Y and Li Y 2003 *Phys. Rev. A* **67** 062504
[54] Yan Z C and Zhang J Y 2004 *J. Phys. B* **37** 1055
[55] Cassar M M and Drake G W F 2004 *J. Phys. B* **37** 2485
[56] Li H, Wu J, Zhou B L, Zhu J M and Yan Z C 2007 *Phys. Rev. A* **75** 012504
[57] Ning Y and Yan Z C 2014 *Phys. Rev. A* **90** 032516
[58] Stephen M J and Auffray J P 1959 *J. Chem. Phys.* **31** 1329
[59] Dalgarno A, Patterson T N L and Somerville W B 1960 *Proc. R. Soc. Lond. A* **259** 100
[60] Kalaghan P M and Dalgarno A 1972 *Phys. Lett. A* **38** 485
[61] Cohen M, McEachran R P and Schlifer I R 1977 *Chem. Phys. Lett.* **49** 374
[62] Ray R D and Certain P R 1977 *Phys. Rev. Lett.* **38** 824
[63] McEachran R P, Veenstra C J and Cohen M 1978 *Chem. Phys. Lett.* **59** 275
[64] Babb J F and Dalgarno A 1991 *Phys. Rev. Lett.* **66** 880
[65] Babb J F and Dalgarno A 1992 *Phys. Rev. A* **46** 5317
[66] Babb J F 1995 *Phys. Rev. Lett.* **75** 4377
[67] Korobov V I, Hilico L and Karr J Ph 2006 *Phys. Rev. A* **74** 040502
[68] Karr J Ph, Bielsa F, Douillet A, Gutierrez J P, Korobov V I and Hilico L 2008 *Phys. Rev. A* **77** 063410
[69] Bakalov D, Korobov V I and Schiller S 2006 *Phys. Rev. Lett.* **97** 243001
[70] Bekbaev A K, Korobov V I and Dineykhan M 2013 *J. Phys. B* **46** 175101
[71] Zhang P P, Zhong Z X and Yan Z C 2013 *Phys. Rev. A* **88** 032519
[72] Korobov V I, Hilico L and Karr J Ph 2009 *Phys. Rev. A* **79** 012501
[73] Luke S K, Hunter G, McEachran R P and Cohen M 1969 *J. Chem. Phys.* **50** 1644
[74] Gersten J I 1969 *J. Chem. Phys.* **51** 3181
[75] Bishop D M and Cheung L M 1977 *Phys. Rev. A* **16** 640
[76] Wolniewicz L and Poll J D 1980 *J. Chem. Phys.* **73** 6225
[77] Wolniewicz L and Poll J D 1985 *Can. J. Phys.* **63** 1201
[78] Moss R E 1993 *Mol. Phys.* **78** 371
[79] Zhong Z X, Yan Z C and Shi T Y 2009 *Phys. Rev. A* **79** 064502
[80] Zhong Z X, Zhang P P, Yan Z C and Shi T Y 2012 *Phys. Rev. A* **86** 064502
[81] Korobov V I and Zhong Z X 2012 *Phys. Rev. A* **86** 044501
[82] Korobov V I, Hilico L and Karr J Ph 2013 *Phys. Rev. A* **87** 062506
[83] Korobov V I, Hilico L and Karr J Ph 2014 *Phys. Rev. Lett.* **112** 103003
[84] Korobov V I, Hilico L and Karr J Ph 2014 *Phys. Rev. A* **89** 032511
[85] Antognini A, Nez F, Schuhmann K, *et al.* 2013 *Science* **339** 417
[86] Gill P 2001 *Science* **294** 1666
[87] Schneider T, Roth B, Duncker H, Ernsting I and Schiller S 2010 *Nature Physics* **6** 275
[88] Karr J Ph, Hilico L and Korobov V I 2011 *Can. J. Phys.* **89** 103
[89] Bhatia A K and Drachman R J 1999 *Phys. Rev. A* **59** 205
[90] Yan Z C and Drake G W F 1996 *Chem. Phys. Lett.* **259** 96
[91] Yan Z C and Drake G W F 1994 *Can. J. Phys.* **72** 822
[92] Harris F E, Frolov A M and Smith V H Jr. 2004 *J. Chem. Phys.* **121** 6323
[93] Stone A P 1961 *Proc. Phys. Soc.* **77** 786
[94] Stone A P 1963 *Proc. Phys. Soc.* **81** 868
[95] Bethe H A and Salpeter E E 1977 *Quantum Mechanics of One- and Two-Electron Atoms* (New York: Plenum)
[96] Pachucki K 2005 *Phys. Rev. A* **71** 012503
[97] Pachucki K and Karshenboim S G 1995 *J. Phys. B* **28** L221
[98] Pachucki K 1998 *J. Phys. B* **31** 3547
[99] Yelkhovsky A 2001 *Phys. Rev. A* **64** 062104
[100] Korobov V I 2004 *Phys. Rev. A* **70** 012505
[101] Kinoshita T and Nio M 1996 *Phys. Rev. D* **53** 4909
[102] Araki H 1957 *Prog. Theor. Phys.* **17** 619
[103] Sucher J 1958 *Phys. Rev.* **109** 1010
[104] Yan Z C 2000 *J. Phys. B* **33** 2437
[105] Bethe H A 1947 *Phys. Rev.* **72** 339
[106] Schwartz C 1961 *Phys. Rev.* **123** 1700
[107] Korobov V I and Korobov S V 1999 *Phys. Rev. A* **59** 3394
[108] Korobov V I 2004 *Phys. Rev. A* **70** 012505
[109] Korobov V I 2006 *Phys. Rev. A* **73** 024502
[110] Korobov V I 2012 *Phys. Rev. A* **85** 042514
[111] Erratum 2012 *Phys. Rev. A* **86** 069905
[112] Drake G W F and Goldman S P 1999 *Can. J. Phys.* **77** 835
[113] Zhong Z X, Yan Z C and Shi T Y 2013 *Phys. Rev. A* **88** 052520
[114] Eides M I, Grotch H and Shelyuto V A 2001 *Phys. Rep.* **342** 63
[115] Eides M I, Grotch H and Shelyuto V A 2007 *Theory of Light Hydrogenic Bound States* (Berlin: Springer)
[116] Korobov V I and Tsogbayar Ts 2007 *J. Phys. B* **40** 2661
[117] Sapirstein J R and Yennie D R 1990 *Quantum Electrodynamics* (ed. Kinoshita T) (Singapore: World Scientific) p. 560
[118] Jentschura U D, Czarnecki A and Pachucki K 2005 *Phys. Rev. A* **72** 062102
[119] Czarnecki A, Jentschura U D and Pachucki K 2005 *Phys. Rev. Lett.* **95** 180404
[120] Erratum 2005 *Phys. Rev. Lett.* **95** 199903
[121] Mohr P J 1975 *Phys. Rev. Lett.* **34** 1050
[122] Mohr P J 1982 *Phys. Rev. A* **26** 2338
[123] Ivanov V G and Karshenboim S G 1997 *Yad. Fiz.* **60** 333
[124] Ivanov V G and Karshenboim S G 1997 *Phys. At. Nuclei* **60** 270
[125] Layzer A J 1960 *Phys. Rev. Lett.* **4** 580
[126] Mohr P J 1983 *At. Data Nucl. Data Tables* **29** 453
[127] Pachucki K 1993 *Phys. Rev. A* **48** 2609
[128] Eides M I, Grotch H and Shelyuto V A 1997 *Phys. Rev. A* **55** 2447
[129] Dowling M, Mondéjar J, Piclum J H and Czarnecki A 2010 *Phys. Rev. A* **81** 022509
[130] Kinoshita T 1990 *Quantum Electrodynamics* (ed. Kinoshita T) (Singapore: World Scientific) p. 218
[131] Laporta S and Remiddi E 1996 *Phys. Lett. B* **379** 283
[132] Eides M I and Grotch H 1995 *Phys. Rev. A* **52** 3360
[133] Melnikov K and van Ritbergen T 2000 *Phys. Rev. Lett.* **84** 1673
[134] Mohr P J, Taylor B N and Newell D B 2008 *Rev. Mod. Phys.* **80** 633
[135] Shen J, Borodin A, Hansen M and Schiller S 2012 *Phys. Rev. A* **85** 032519
[136] Drullinger R E, Wineland D J and Bergquist J C 1980 *Appl. Phys.* **22** 365
[137] Larson D J, Bergquist J C, Bollinger J J, Itano W M and Wineland D J 1986 *Phys. Rev. Lett.* **57** 70
[138] Baba T and Waki I 1996 *Jpn. J. Appl. Phys.* **35** L1134
[139] Drewsen M, Jensen I, Lindballe J, Nissen N, Martinussen R, Mortensen A, Staanum P and Voigt D 2003 *Int. J. Mass Spectrom.* **229** 83
[140] Willitsch S, Bell M T, Gingell A D and Softley T P 2008 *Phys. Chem. Chem. Phys.* **10** 7200
[141] Baba T and Waki I 2002 *J. Appl. Phys.* **92** 4109
[142] Schiller S and Lämmerzahl C 2003 *Phys. Rev. A* **68** 053406
[143] Tong X, Winney A H and Willitsch S 2010 *Phys. Rev. Lett.* **105** 143001
[144] Tong X, Wild D and Willitsch S 2011 *Phys. Rev. A* **83** 023415
[145] Mackenzie S R, Merkt F, Halse E J and Softley T B 1995 *Mol. Phys.* **86** 1283
[146] Willitsch S and Merkt F 2005 *Int. J. Mass Spectrom.* **245** 14
[147] Roth B, Koelemeij J C J, Daerr H and Schiller S 2006 *Phys. Rev. A* **74** 040501